MEASURING AND ANALYZING JOINT ACOUSTIC EMISSIONS FROM THE WRIST

A Dissertation
Presented to
The Academic Faculty

by

Daniel Hochman

In Partial Fulfillment
of the Requirements for the Degree
Master of Science in the
School of Mechanical Engineering

Georgia Institute of Technology
May 2021

MEASURING AND ANALYZING JOINT ACOUSTIC EMISSIONS FROM THE WRIST

Approved by:

Dr. Omer Inan, Advisor
School of Electrical and Computer Engineering
Georgia Institute of Technology

Dr. Aaron Young, Co-advisor
School of Mechanical Engineering
Georgia Institute of Technology

Dr. Woonhong Yeo
School of Mechanical Engineering
Georgia Institute of Technology

Date Approved: April 15, 2021

ACKNOWLEDGEMENTS

I would first like to thank my research advisor, Dr. Omer Inan. Without his wealth of knowledge, thoughtfulness, and excellent leadership, none of the following work would have been possible. I would also like to thank Dr. Woonhong Yeo and my co-advisor, Dr. Aaron Young for your willingness to assess my work as members of my reading committee.

I need to also thank everyone in the Inan Research Lab. I feel truly honored to have worked in such a productive and selflessly collaborative working environment. Specifically, I would like to thank Brandi Nevius, Caitlin Teague, Daniel Whittingslow, Mohsen Safaei, Nick Bolus, and Sevda Gharehbaghi for laying a foundation for my work and teaching me everything I needed to know to begin. I would also like to specifically thank Göktuğ Özmen for working closely with me in development and being available to bounce ideas off. Our conversations have been stimulating and enlightening.

Finally, I must express my deepest gratitude to my family for loving and supporting me in all I have ever hoped to do since before I can remember, and my girlfriend, Jodi, who moved from Madison to Atlanta to be with me while I pursued my education. I can only hope to be able to return the same level of love and commitment to all of you.

TABLE OF CONTENTS

LIST OF TABLES

LIST OF FIGURES

LIST OF SYMBOLS AND ABBREVIATIONS

ADC	Analog-to-Digital Converter
AFE	Analog Front-End
CI	Confidence Interval
CT	Computed Tomography
CV	Coefficient of Variability
CCW	Counter-Clockwise
CW	Clockwise
DAQ	Data Acquisition Unit
EMR	Electronic Medical Record
FE	Flexion-Extension
FSR	Force Sensitive Resistor
GRRAS	Guidelines for Reporting Reliability and Agreement Studies
ICC	Intraclass Correlation Coefficient
IMU	Inertial Measurement Unit
JAE	Joint Acoustic Emission
JIA	Juvenile Idiopathic Arthritis
JS	Jensen-Shannon
KL	Kullback–Leibler
LED	Light Emitting Diode
Mic	Microphone
microSD	Miniaturized Secure Digital Card
MRI	Magnetic Resonance Imaging

NSF	National Science Foundation
PCB	Printed Circuit Board
PLA	Polylactic Acid
SEm	Standard Error of Measurement
SNR	Signal-to-Noise Ratio
USB	Universal Serial Bus

SUMMARY

Joint acoustic emissions (JAEs) measured from the knee present promise as a method of noninvasive knee health quantification. This work adapts the methods developed for knee JAE measurements to the wrist – another joint commonly afflicted with injuries and degenerative disease. First, JAEs are measured using contact microphones at eight locations around the wrist during prescribed exercises (wrist flexion-extension and rotation) to find reliable and consistent wrist JAE measurement methods. The benchtop measurement setup established for knee JAE measurements is directly incorporated in this study. JAE signal strength is assessed using the signal-to-noise ratio (SNR). Then, nine features that have shown importance in JAE analysis are extracted, and the intraclass correlation coefficient (ICC) (model 3,*k*), coefficients of variability (CVs), and Jensen-Shannon (JS) divergence are used to assess the interrater and intrarater repeatability, revealing both exercises produce JAEs and three locations demonstrated high JAE signal strength and repeatability. Second, a wrist wearable system is developed for high quality JAE sensing. Low-profile wide-band analog accelerometers to measure and analyze JAEs from two reliable locations on the wrist are sampled and saved on a microSD using a custom-designed printed circuit board. Using custom-developed casings, one accelerometer is clipped to the loop of a watchband for placement on the radius and the other is contained in a custom-developed grip for placement against the palm. Proper grip strength is reinforced in real time using a force sensitive resistor and light emitting diodes. A flex sensor is secured along the volar side of the wrist for synchronously tracking wrist motion for improved cycle-by-cycle JAE analysis. This wrist wearable JAE sensing system

is validated using SNR, ICC, CV, and JS divergence and compared to the benchtop setup. The developed wearable system is critical in moving toward monitoring wrist JAEs for at-home wrist joint health assessment.

CHAPTER 1. INTRODUCTION

Musculoskeletal injuries and degenerative disease are a huge burden on society today, where as many as 1 in 4 people across age groups and cultures report chronic musculoskeletal pain [1]. These conditions are a leading cause of missed workdays, reduce quality of life, and are a major financial burden on health systems [2]. Standard noninvasive examination methods include subjective measures and expensive imaging. Treatment tracking quickly compounds the cost of these conditions, as repeated imaging may be prohibitively expensive and repeated visits to the clinic increase missed days of school or work. Additionally, a shortage of pediatric rheumatologists means only 1 in 4 children diagnosed with Juvenile Idiopathic Arthritis (JIA) is able to regularly see a pediatric rheumatologist [3], [4]. These factors, as well as the increased reliance on telemedicine during the ongoing pandemic, necessitate the presence of a noninvasive joint health measurement technique which can facilitate physical examination of joint health in a remote setting.

Recent work has demonstrated that the vibration at the surface of the skin caused by dynamic interactions within a joint during articulation [5], commonly referred to as “joint sounds” or “joint acoustic emissions” (JAEs), can be used as a quantitative measure which can be employed to inform joint health. These works have been able to discriminate between healthy and injured [6]–[9], healthy and arthritic [4], [10]–[17], and loaded and unloaded knees [17], [18]. Using characteristics of JAEs as a potential digital biomarker of joint health shows great promise as an avenue for introducing joint health monitoring to an at-home environment. However, most of the research in JAE monitoring has focused on

the knee because it is the largest joint in the human body and has a huge impact on the population, with 18 million annual clinical visits attributed specifically to knee pain [19]. The wrist joint is also commonly afflicted with injuries and degenerative disease. It is therefore necessary to assess whether techniques for JAE measurement can be developed for the wrist, but to the best available knowledge, no work had previously been done in capturing JAEs from the wrist.

The aim of this work is to expand the field of research on JAEs to the wrist joint. First, it is important to determine whether JAEs can be reliably extracted from the wrist. Many studies investigating JAEs of the knee utilize contact microphone (mic) placement locations 2 cm medial and lateral to the patellar tendon as reliable locations for extracting JAEs from the knee [20]. Therefore, a mic placement location or set of locations which can reliably extract wrist JAEs must be identified. Previous studies on knee JAEs have also explored the effect of different exercises on producing meaningful passive JAEs [17], [18], [21]. A study of wrist JAEs should also identify the exercises which can repeatably produce JAEs. This is investigated by using a benchtop system that has been validated to reliably extract meaningful JAEs from the knee [4], [9], [17], [22] to record JAEs from healthy volunteers' wrists [23] performing two separate exercises at eight anatomically and experimentally determined locations around the wrist [24]. Signal strength and repeatability measures [7], [21] of nine spectral and temporal features important to JAE analysis are evaluated to assess wrist JAE recording quality and reliability.

Once repeatable wrist JAE extraction techniques are established, a novel wearable device for improved wrist JAE extraction is developed. The wearable device employs a miniaturized version of a circuit designed specifically for untethered capturing of knee

JAEs [25], two contact microphones, a sensor for tracking the motion of the wrist, a sensor for validating that proper mic contact force against the skin is maintained [22], [26], and the mechanical hardware necessary to secure all sensors in the desired locations on the wrist for the high quality wrist JAE measurement. To reinforce proper user input for optimal JAE production and recording, microphone contact force feedback is given real time using red and green light emitting diodes (LEDs) and motion guidance animations alongside real time motion tracking feedback were implemented. The performance of the wearable device is assessed by comparing JAE signal quality and repeatability to the same measures from the previously validated benchtop system. These measures are then analyzed to confirm the viability of the wearable JAE sensing device for use in clinical joint health monitoring studies. Findings of this research will lay a foundation for convenient and reliable non-invasive wrist joint health assessment in uncontrolled settings using JAE analysis within a wrist wearable form factor.

CHAPTER 2. BACKGROUND

2.1 Overview

The wrist is a complex joint which allows for multiple axes of motion and is often subject to damage via injury or degenerative disease. Common clinical assessment techniques are invasive, subjective, or expensive, and repeated clinic visits for diagnosis and treatment tracking may not be feasible for many patient populations. The analysis of JAEs has shown promise as a quantitative measure for diagnostic and treatment tracking aid, and it is possible to capture JAEs in a wearable form factor, offering the opportunity to improve access to care from an at-home setting. The wrist offers an exciting possibility in the development of wearable JAE monitoring technology with an unobtrusive form factor which could expand the benefits offered by JAE monitoring technology to a larger population.

2.2 Wrist Joint Pathology and Assessment Techniques

The wrist endures heavy use during athletic activities and is therefore often subject to injuries from overuse or trauma, including within juvenile populations. Approximately 1.3% of all adolescents who participate in athletics are afflicted with wrist injuries caused either by trauma in contact sports or overuse in golf, gymnastics, and racquet sports [27]. Overall, the hand and wrist combine as the third most commonly injured body part in the United States [28]. Wrist joint involvement is also common in those affected with degenerative joint diseases. As many as one in seven people in the US has some form of arthritis of the wrist [29]. Wrist arthritis also affects juvenile populations, as 34% of

children with JIA report wrist impairment, and 15-23% of that population shows active arthritis of the wrist [30]. Injuries and diseases of the wrist joint reduce quality of life, add to healthcare costs, and account for a huge impact on missed workdays [28]. The total economic impact of these injuries places them as the most expensive injury group at a population level [31]. Standard practice in the noninvasive diagnosis and treatment tracking of such conditions involves a combination of subjective measures such as patient reported symptoms, mobility assessments, physical examinations, and expensive imaging procedures such as x-rays, computed tomography (CT), and magnetic resonance imaging (MRI) [32]. More invasive procedures like arthroscopy of the wrist are also used for improved diagnostic power and treatment of some wrist ailments [33]. Because these procedures are costly, repeated clinic visits to track the progress of one's treatment can become prohibitively expensive, leaving subjective pain assessments as a primary tracking tool for remote care. Therefore, there is a need for improved at-home wrist joint health monitoring using quantitative, rather than qualitative, measurement techniques.

2.3 Wearable Health Monitoring

Numerous physiological phenomena from the body emit signals which can be detected by sensors. Such signals have been a subject of research for centuries. In recent years, the miniaturization of sensors and electronics has allowed for some of these signals, such as cardiac rhythm [34], activity [34], [35], and blood oxygen saturation [36], to be monitored passively with noninvasive wearable technology. These may take various form factors, including patches that attach to the skin [37], sensors embedded in clothing [38], wrist watches [39], smartphone applications [40], and more. These wearable devices allow for passive health monitoring more frequently than would be possible in a clinical setting,

improving the likelihood of catching diseases which may not present during a clinic visit [37]. Additionally, the rise in patient-accessible electronic medical records (EMRs) allows for the data from these wearable sensors to be sent to healthcare providers so providers may monitor their patients in a telehealth setting [41], expanding access to care, empowering patients with their own health, and reducing the burden on healthcare providers.

2.4 Joint Acoustic Emission Sensing

2.4.1 JAE Sensing Techniques

JAEs were first described by Blodgett in 1902. Using an off-the-shelf stethoscope pressed against the knee in motion, he noted the sounds produced by dynamic interactions within the joint and estimated that clinically relevant information is contained within those sounds [5]. Although in-air microphones may sense JAEs when placed near an articulating joint, the impedance mismatch between the skin and air makes the use of contact microphones (mics) and stethoscopes more practical for high quality JAE sensing [8]. Therefore, though JAEs have been known to science for over a century, JAE sensing methods within a wearable form factor did not become feasible until the creation of accelerometers and piezoelectric devices which could be fixed to the skin unobtrusively. The recent emergence of low-profile high-bandwidth contact microphones has increased motivation for further research into JAEs. Now, the analysis of audio measurements from JAE recordings shows promise as a biomarker for joint health, as recent studies on JAEs from the knee have demonstrated the ability to differentiate between healthy and injured [6]–[9], healthy and arthritic [4], [10]–[17], and loaded and unloaded knees [17], [18].

These studies have applied a wide range of signal processing techniques to JAE recordings to distinguish between healthy and ailing, or unloaded and loaded knees, but there are also many commonalities within the methods of acquiring JAE signals to allow for optimal analysis. First, the structures within the knee must create dynamic interactions to produce JAEs. To do this, past studies have often employed unloaded knee flexion-extension (FE), but have also explored using exercises which introduce a higher load on the knee, including sit-to-stand, squat, stair climb, and vertical leg press [4], [16]–[18]. The interactions produced by these exercises creates JAEs which then need to be recorded. High bandwidth and low-profile contact microphones are commonly used for the detection of the low frequency grinding [26] and high frequency clicking [11] sounds characteristic of JAEs. These mics need to be secured to the skin on the desired location of the joint in a manner that will minimize any motion artifacts from rubbing against skin [26]. Adding a consistent light backing force is also desired to improve the sensing performance of the mic [22] and reduce the inter-trial and inter-user variability of JAE recordings [26]. Recording the applied backing force also allows for identification of any occurrences where the mic breaks contact with the skin [26] and allows for analysis of time-segments where low frequency signal is filtered out because too much contact force is applied or high frequency signal is filtered out from too little backing force [22]. Synchronous tracking of the joint angle allows for back-end analysis to be performed on a cycle-by-cycle basis, which has proven helpful [4] due to the cyclical nature of JAE production during motion cycles [8].

Researchers have proposed some different approaches in JAE recording signal processing. However, a general pattern in the processing of JAE recordings is as follows.

JAE recordings are filtered to exclude as much thermal noise and motion artifact as possible without sacrificing much of the frequency band of JAEs [9], [10], [22], [26]. Audio recordings are then broken into motion cycles based on synchronous joint angle recordings [4], [8], [10], [17], [18], [25]. Cycles with strong definitive motion artifacts can then be discarded. Each remaining cycle is then broken up into windows of specified length and overlap. Then, distinct spectral features [4], [10], [17], temporal features [4], [10], b-value [9], [42], and other features, are extracted from each window. These features are then often fed into a supervised [4], [10], [17] or unsupervised [7], [18] machine learning model to derive clinically relevant regression or classification.

2.4.2 The Wrist as a Target Joint for JAE Sensing

The combination of the rate of pathology that affects the wrist and the platform which the wrist provides for wearable systems dictates that the wrist is a logical choice to expand JAE research to new joints. However, to the best available knowledge, JAEs have minimally been studied around the wrist. This necessitates a study to indicate whether wrist JAEs can be reliably extracted from a wrist in motion similar to knee JAEs [21].

The wrist is an ellipsoid joint capable of motion in more than two planes [43]. The dynamic interactions which produce JAEs may be created within the intercarpal joints via a combination of FE, radial-ulnar deviation, and circumduction (rotation). Adding weights would increase the load on the joint to further increase the interactions within the joint that create JAEs [18]. Due to smaller range of motion compared to knee, such exercises can be performed in two second cycles to create a repeatable procedure for JAE production as opposed to four second cycles commonly prescribed for knee JAE excitation. The

structural complexity of the wrist joint means that there may be many potential skin surface locations to monitor JAEs, either via a soft tissue pathway from the intercarpal joints to the skin surface or via sound conduction along a bone. The wrist joint may be described as a curved line between the styloid processes of the radius and ulna, curving proximally 1 cm [44]. Three potential proximal mic locations (P1–P3) are 3 cm proximal to the wrist joint with the first centered between the radius and ulna on the dorsal side, the second centered between the radius and ulna on the volar (palmar) side, and the third on the skin covering the radius. The first and second locations were selected because the soft tissue in the region allows for a relatively unobstructed path for vibration to propagate from the wrist, whereas the third location allows for sound conduction along the radius [45]. These locations are also optimal locations for a wristwatch-style wearable design and have minimal skin motion relative to the underlying skeletal structure [46], [47], which should minimize motion artifact production. Two potential distal locations for mic placement are each 3 cm distal to the wrist joint, where one (D1) is centered between the second and third metacarpal bones on the dorsal side, and another (D2) is centered between the first and second metacarpal bones on the palmar side. These were selected for proximity to the distal end of the carpal bones, the soft tissue pathway for JAEs to travel unobstructed [45], and the small amount of skin motion relative to the underlying bone structure [46], [47]. D2 also provides the ability to listen to wrist JAEs through a custom-designed grip, a potential design for an at-home joint health monitoring system. Three potential middle mic locations (M1–M3) are all on the wrist joint, where M1 is 1 cm distal to the dorsal tubercle, M2 is distal and adjacent to the radial styloid process, and M3 distal and adjacent to the ulnar styloid process. These locations were selected for their location on the wrist joint with a

soft tissue pathway for JAE propagation [45]. Skin motion is high in these locations relative to the underlying skeletal structure [46], [47]. Thus, motion artifacts within the signals, characterized as high signal power without the grinding or clicking sounds characteristic of JAEs, are expected. Other mic placement locations are possible but are not described, either to prevent redundancy or because of poor performance during preliminary experimentation. Assessing the signal strength and repeatability of wrist JAE monitoring from the locations and exercises detailed above will confirm whether it will be feasible to study wrist JAEs and develop wearable technology to monitor them to expand availability of quantitative wrist joint health monitoring to clinical and at-home settings.

2.4.3 Design Requirements of JAE Sensing Systems

Systems for monitoring JAEs have been under constant development in recent years. One of the earlier systems developed specifically for JAE monitoring was implemented by Töreyin et al. This system used airborne microphones for acoustic monitoring of knee JAEs and accelerometers for tracking joint angle [48]. Since then, acoustic measurement techniques have evolved to use contact microphones [20], employ various joint angle measurement techniques including more advanced inertial measurements extracted from multiple IMUs, and have even moved to untethered systems [25]. However, there is a consistent set of requirements for JAE monitoring systems. First, the system must employ sensors for acoustic measurement. Most recently, this has meant placing high sensitivity contact microphones on the skin at specific anatomical locations around the joint known for reliable JAE extraction [22], [26] using placement methods which minimize the introduction of motion artifacts, maximize the measured JAE signal strength and repeatability, and don’t filter out frequency ranges important to JAE analysis

[22], [26]. These sensors must then be sampled by electronics at a high enough frequency such that the upper end of the frequency spectrum of JAEs is much less than the Nyquist frequency. Second, JAE measurement techniques must also track the motion of the joint to validate JAEs are cyclical with the motion of the joint [20] and improve data segmentation capabilities [4], [8], [10], [17], [18], [25]. Lastly, the acoustic measurements and joint angle tracking data must be saved for later analysis.

There are additional requirements when developing a wearable system for JAE monitoring. Such systems require additional electronic considerations such as power-consumption, sample rate, battery life, data storage capacity, a data transfer method (to a computer), and printed circuit board (PCB) design [25], [49]. They must also be small enough to be secured near the joint unobtrusively, fit people of various sizes, and have mechanisms of securing the system to the joint without negatively impacting the performance of the electronic systems [50]. For wide adoption, they should also be inexpensive and simple to use [49]. Systems which are wrist wearable may also have added requirements knee-wearable systems do not have. The knee is restricted to a single axis of motion, but the wrist may move in two [43]. A wrist wearable JAE sensing system must not restrict either axis of motion. Additionally, joints in close proximity to the wrist, such as those which allow finger motion, may create artifacts unrelated to wrist motion within the acoustic signal, and should therefore be immobilized. Wearables developed for pediatric settings also introduce their own design constraints. Children are small, so the wearable design must be less obtrusive than a wearable device designed for adults. The design of a wearable in pediatric settings must also be highly decorative, and user input must be simple and appealing.

CHAPTER 3. ASSESSING THE REPEATABILITY OF JAE MONITORING AROUND THE WRIST

Research around JAEs has almost entirely focused on analyzing JAEs of the knee. This work aims to utilize similar techniques to those which have been established around knee JAE extraction techniques to establish a framework for wrist JAE measurement and analysis. Once this is established, technology for wearable wrist JAE monitoring in clinic or at-home can be developed and deeper research into the clinical relevance of wrist JAEs can commence.

3.1 Methods

3.1.1 Study Design and Ethics

This study follows the Guidelines for Reporting Reliability and Agreement Studies (GRRAS) [51]. All human subjects research was conducted under approval by the Georgia Institute of Technology Institutional Review Board (#H15398). Volunteers provided written informed consent prior to participation in the study.

3.1.2 Participants

Seven healthy college-aged volunteers (three male/four female, 24.9 ± 3.5 years, 65.3 ± 8.4 kg, and 168.0 ± 10.1 cm) were recruited. Inclusion criteria for participation in this study dictated volunteers must have no history of major wrist injury or degenerative joint disease. Additionally, if volunteers had changes to wrist joint health between recording sessions, they would be excluded from the study. No volunteers met this

exclusion criteria, so no such exclusions were made. Other factors which may affect wrist JAEs such as volunteers' daily medication usage, day-to-day wrist activity levels, and history of previous minor wrist injuries were not controlled. An additional volunteer who had juvenile idiopathic arthritis (JIA) as a child (female, 41 years, 75 kg, 175 cm) was included to facilitate proof-of-concept qualitative comparisons to the healthy volunteers and to allow the development of hypotheses for future studies to investigate.

A previously recorded dataset (seven male/three female, 25.1 ± 2.9 years, 72.4 ± 13.4 kg, and 170.1 ± 13.4 cm, no history of major knee joint injury or degenerative disease, 5-10 motion cycles each) of JAE recordings from knee squat exercises recorded at sites 2 cm medial and lateral to the patellar tendon on both legs of college-aged individuals was used to compare the signal strength measurements of wrist JAE recordings against the two locations on the knee known to provide salient knee health assessment. The same data acquisition system [52], pre-processing steps, and signal strength assessment methods were used in this dataset as were used in the wrist recordings to ensure consistency in methods to provide a valid comparison.

3.1.3 Experimental Protocol

On each day of study participation, volunteers moved their wrists around at random for 20-30 s to precondition their wrists and remove artifacts caused by crepitus. Volunteers then practiced the prescribed 2 s period wrist FE and rotation exercises alongside animations designed to provide guidance in these exercises. Here, radial-ulnar deviation is excluded from the set of prescribed exercises due to poor ability to elicit JAEs in preliminary experiments, and weighted conditions are excluded because unweighted

exercises sufficiently produced desired JAEs. Mics were secured to four of the eight locations around the wrist described in 2.4.2 and shown in Figure 1 using double-sided craft tape (Elizabeth Craft Designs, Evergreen, CO, USA). JAEs were then recorded while the volunteers performed 10 exercise cycles, again following the provided animations, three times for each combination of unweighted FE and rotation exercises at two sets of microphone location for both wrists. Volunteers performed this protocol on each of two separate days, separated by less than a week.

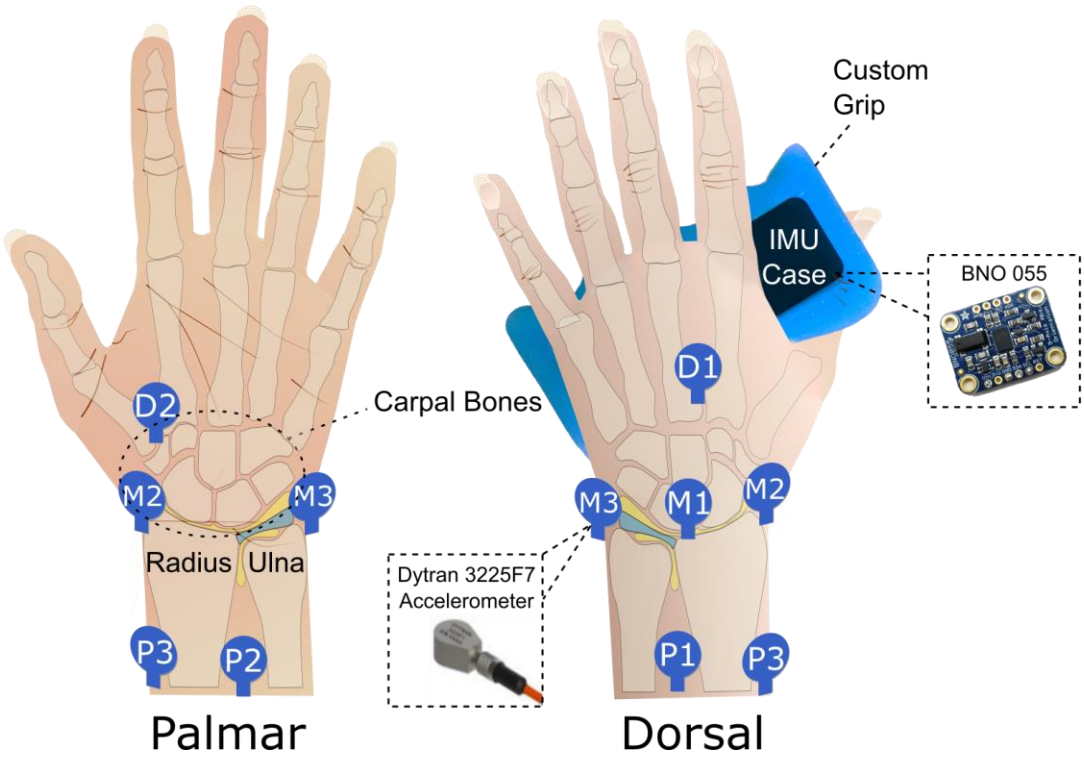

Figure 1: Testing setup for recording joint acoustic emissions (JAEs) from the wrist. During a recording, the wrist has accelerometers (either P1–P3 and D1 or M1–M3) attached to the skin with double sided tape. The volunteer holds the grip which contains the inertial measurement unit (IMU) and an accelerometer to press against the skin at location D2. The data from the four accelerometers were synchronously recorded via a National Instruments data acquisition unit, which was controlled by a computer running MATLAB.

3.1.4 Signal Extraction, Signal Processing, and Signal Strength Assessment

The JAE sensing system employed in this study consists of four miniature uniaxial accelerometers (Series 3225f7, Dytran Instruments, Inc., Chatsworth, CA, USA) with wide bandwidth (2 Hz–60 kHz), and high sensitivity (100 mV/g). These accelerometers, used as contact microphones, were fixed to the skin using double-sided tape. The other end of the accelerometers was connected to a computer via input channels a data acquisition unit (DAQ) (USB-4432, National Instruments, Austin, TX, USA) [52], which were sampled at a rate of 50 kHz, and saved for subsequent processing using scripts in MATLAB (MathWorks, Natick, MA, USA).

An inertial measurement unit (IMU) (BNO055, Adafruit Industries, New York, NY, USA) was connected to a microcontroller (UNO, Arduino, Somerville, MA, USA) to monitor the motion of the wrist joint relative to the forearm while volunteers performed the wrist exercises necessary to excite JAEs. To best track wrist motion, the forearm was held stationary by strapping it to the arm of the volunteer's chair and the IMU had to be held in the hand of the wrist in motion. A custom grip (shown in Figure 1) made of silicone gel (Ecoflex GEL, Smooth-On, Easton, PA, USA) was developed with slots designed to fit the accelerometers and a custom-developed IMU case, allowing volunteers to hold the IMU, press the accelerometer onto the skin of the palm, and prevent extraneous finger motion. The combination of the broad bandwidth mics to pick up JAEs and an IMU to track kinematics creates a framework for monitoring JAEs from the wrist in motion.

The first step in processing the raw audio signal is applying a Kaiser window bandpass filter (150 Hz–20 kHz). At this point, qualitative analysis is performed by visually

comparing the filtered waveforms and listening to the sounds recorded by the microphones of all healthy volunteers who had no history of major wrist injury or illness to the recordings from the volunteer who has a history of JIA from childhood and audible wrist JAEs. An example of such qualitative comparisons can be demonstrated with the signals shown in Figure 2.

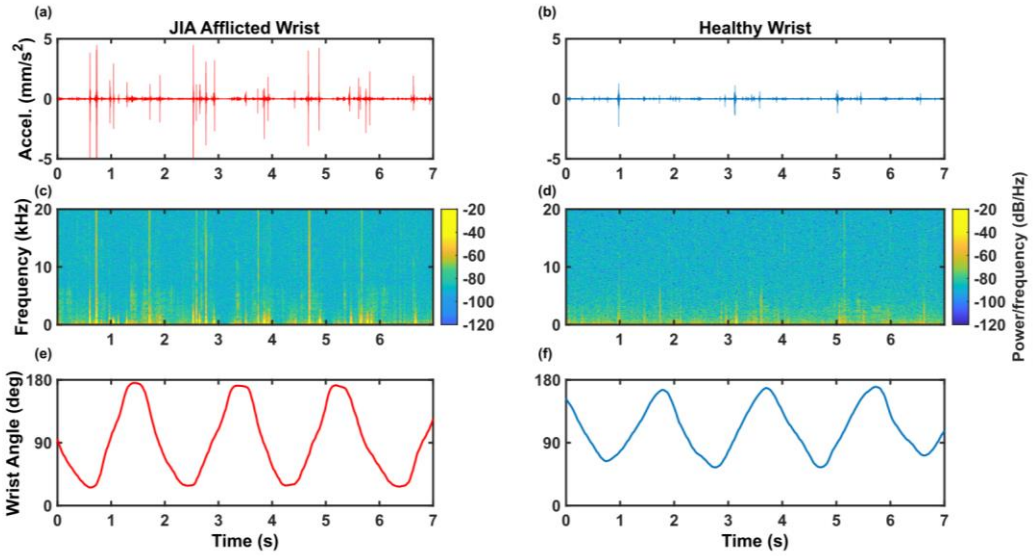

Figure 2: (a,c,e) Volunteer who was afflicted with juvenile idiopathic arthritis (JIA) as a child and continued to have audible JAEs from the wrist during articulation. (b,d,f) Volunteer with no history of wrist pathology. (a,b) Time domain of acoustic signal from the wrist. (c,d) Spectrogram of the acoustic signal displayed above it. (e,f) Motion data from the IMU recorded synchronously with the acoustic signal.

Once the presence of JAEs was confirmed within the dataset of healthy volunteers, the microphone signal is segmented into the 10 movement cycles of prescribed motion using the IMU signal. Each cycle is windowed into 400 ms long frames with 50% overlap [4], [17], and nine spectral and temporal features (zero-crossing rate, acoustic energy, spectral centroid, spectral spread, spectral flux, harmonic ratio, spectral crest, spectral decrease, and spectral slope) are extracted for the statistical analysis. These raters were

selected in a review of previous studies able to separate healthy joints and joints afflicted with degenerative disease [4], [10], [17], [21] based on their relative importance within the respective machine learning models. The measurements and raters in this experiment are not calculated independently.

To assess the effects of the unwanted noise and motion artifacts at each location, the signal-to-noise ratio (SNR) was calculated as follows. First, the Teager energy operator finds the characteristic JAE clicks in the signal, chosen as the peaks greater than 20% of the range of the signal value, as has been proven to be successful in JAE analysis by Semiz et al. [11]. Click windows were categorized as the time ± 50 ms of each detected click. The remaining signal recordings are classified as the windows of noise and motion artifacts. The power of each window is calculated, and the ratio of power of the click windows taken against the power of the motion artifact windows yields a SNR measurement for each recording. These are summarized by location to assess the signal strength relative to the motion artifacts at each microphone placement location and for each exercise.

3.1.5 Statistical Analysis

All statistical analysis is performed using scripts in MATLAB. The mean, median, and standard deviation of the features of all windows are calculated and stored as a vector of features for each cycle, where there are 60 such feature vectors for each combination of volunteer, wrist, exercise, and location (six sessions of 10 cycles each). The average of each feature over those 60 vectors is calculated to give a single averaged feature vector for each combination of volunteer, wrist, exercise, and location.

The intraclass correlation coefficient (ICC) is a widely used metric of measurement reliability across different raters [4] and has been used successfully in previous JAE repeatability tests [20], [21], [26]. Using ICC to describe intersession reliability, each feature vector acts as a measurement where every feature is a rater. The two-way mixed effects, consistency, multiple raters/measurements model of ICC (model 3,*k*) is used to calculate interrater ICC values with a 95% confidence interval (CI) [53]. All measurements at each location were used to calculate the ICC for each location. Likewise, all measurements for each exercise are used to calculate the ICC for the two exercises. Intrasession reliability is calculated using the same ICC calculation methods as for intersession reliability, where the two separate days of recordings for each volunteer represented different measurements; thus, there are twice as many feature vector measurements for ICC calculations. ICC values were assessed according to Fleiss [54], where values less than 0.40 are "poor", values between 0.40 and 0.75 are "fair to good", and values greater than 0.75 are "excellent". These values are presented at a high level among all volunteers. To assess the variability between volunteers, ICC is also calculated on a volunteer-by-volunteer basis and the standard deviation of the ICC calculation between volunteers at each location is reported.

JS divergence is a symmetrical variant of the Kullback–Leibler (KL) divergence, which measures the entropy between two probability distributions that are meant to represent the same dataset to confirm the measurement consistency [55], [56]. To find the JS divergence, distributions of each feature are needed: the nine features calculated for each bin are kept such that they could be summarized as a histogram of the feature distribution for each recording of 10 cycles. Then, the average distribution of similar

recordings on a recording date (all recordings from the same session date, volunteer, wrist, exercise, and location) is taken. The KL divergence of each of those similar recordings is calculated using the averaged distribution as the "ground truth recording" [55], [56]. Averaging these KL divergence values gave the intrasession JS divergence of each feature for that combination of session date, volunteer, wrist, exercise, and location. JS divergence is then summarized by location and exercise [56].

The standard error of measurement (SEm) is found for both JS divergence and SNR calculations. The SEm is then multiplied by 1.96 to give a confidence bound, which is added to the top and bottom of the measurement (JS Divergence or SNR) to give a 95% CI. The coefficient of variation (CV) is also calculated for each feature at each location and exercise to assess intrarater variability, where low levels of variation are defined as CV values less than 12% [21].

3.2 Results

3.2.1 Reliability Measurements

The calculated intrasession ICC values with 95% CIs for FE and rotation exercises over all tested locations are displayed in Table 1. Intersession ICCs with 95% CIs for FE and rotation exercises over all tested locations are displayed in Table 2. Standard deviation of intrasession ICC between volunteers is 0.082 for both exercises, and standard deviation of intersession ICC between volunteers is 0.091 for both exercises. Intrarater repeatability analysis using intrasession JS divergence (values closer to 0 indicate high levels of similarity) on the nine identified features extracted from the filtered acoustic signal gives median JS divergence of 0.190 (95% CI of 0.186–0.193) for FE and 0.187 (95% CI of

0.184–0.190) for rotation. Assessing the variation of feature values for each exercise yields mean CV values displayed in Table 1 and Table 2.

Table 1. Intrasession intraclass correlation coefficients (ICC) values with 95% confidence intervals and coefficient of variation (CV) evaluated for all tested exercises and at all tested locations around the wrist.

	Intrasession Reliability			
		95% CI		
	ICC	Lower Bound	Upper Bound	CV
Flexion-Extension	0.632	0.478	0.758	0.161
Rotation	0.820	0.745	0.881	0.107
Location P1	0.631	0.477	0.757	0.156
Location P2	0.752	0.649	0.836	0.152
Location P3	0.847	0.784	0.899	0.153
Location D1	0.811	0.734	0.875	0.157
Location D2	0.837	0.770	0.892	0.143
Location M1	0.849	0.787	0.900	0.099
Location M2	0.857	0.798	0.905	0.101
Location M3	0.872	0.819	0.915	0.109

Table 2. Intersession ICC values with 95% confidence intervals and CV evaluated for all tested exercises and at all tested locations around the wrist.

	Intersession Reliability			
		95% CI		
	ICC	Lower Bound	Upper Bound	CV
Flexion-Extension	0.631	0.525	0.723	0.236
Rotation	0.789	0.729	0.841	0.183
Location P1	0.629	0.399	0.801	0.225
Location P2	0.760	0.614	0.871	0.241
Location P3	0.847	0.754	0.917	0.233
Location D1	0.817	0.706	0.902	0.231
Location D2	0.840	0.743	0.914	0.232
Location M1	0.855	0.768	0.922	0.169
Location M2	0.870	0.791	0.930	0.170
Location M3	0.886	0.817	0.938	0.176

Intrasession ICC with 95% CIs for all locations are shown in Table 1. The intersession ICC with 95% CIs for all locations are shown in Table 2. The standard deviation of intrasession ICC across volunteers is 0.078 at location P1, 0.040 at location P2, and between 0.001 and 0.009 for locations P3, D1, D2, and M1–M3, and the standard deviation of intersession ICC across volunteers is 0.116 at location P1, 0.025 at location P2, and between 0.002 and 0.005 for locations P3, D1, D2, and M1–M3. Performing similar repeatability analysis using intrasession JS divergence on these locations gives median values between 0.18 and 0.20 (with 95% CIs in the same range). Assessing the variation of feature values for each location yields mean CV values shown in Table 1 and Table 2.

3.2.2 Signal Strength

Assessing the signal strength relative to noise level after filtering, the median SNR is 6.0 dB (95% CI of 5.8–6.2 dB) for FE and 6.1 dB (95% CI of 5.7–6.5 dB) for rotation with standard deviation between volunteers of 1.9 dB for FE and 1.0 dB for rotation.

SNR values for summarized by location yields Figure 3. Here, it can be demonstrated that over all volunteers, locations P1–P3 have higher median SNRs (9.8 with 95% CI of 8.6–10.9, 7.4 with 95% CI of 6.7–8.0, and 7.4 with 95% CI of 6.8–8.0 dB, respectively) than other locations ($p < 0.001$, using two-sample t-test with Bonferroni correction). Locations D1, D2, and M1–M3, where median SNRs are 4.5 (95% CI of 3.6–5.3), 5.6 (95% CI of 4.9–6.3), 4.1 (95% CI of 3.6–4.7), 4.2 (95% CI of 3.5–4.9), and 6.3 (95% CI of 5.7–6.9) dB, respectively. Additionally, the standard deviation of SNRs between volunteers ranges from 1.6 to 2.5 dB. The dataset of recordings from knee squats of healthy volunteers shows a median SNR of 5.5 (95% CI of 4.8–6.3) dB at 2 cm medial

to the patellar tendon and a median SNR of 7.2 (95% CI of 6.6–7.9) dB 2 cm lateral to the patellar tendon.

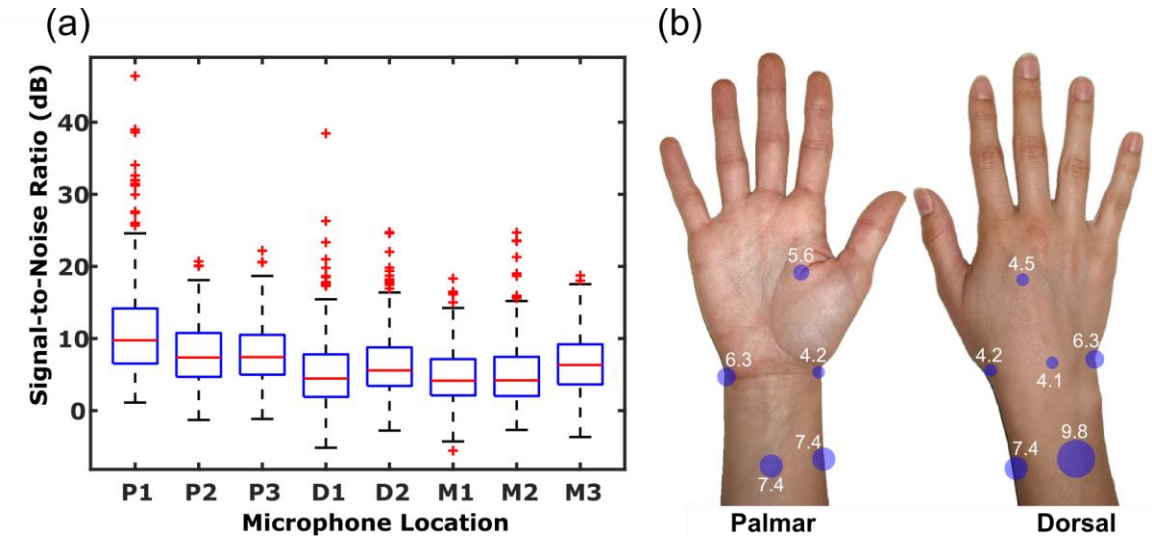

Figure 3: (a) Box-and-whisker plot of signal-to-noise ratio (SNR) measurements at each microphone placement location after filtering with a Kaiser-window bandpass filter using a passband of 150 Hz–20 kHz. (b) SNR is displayed as circles centered at the microphone location that SNR was measured at. SNR (dB) is represented as the radius of the circle and median SNR values are displayed beside the circles.

3.3 Discussion

3.3.1 Evaluating the Ability of Prescribed Exercises to Excite Joint Sounds

Recordings taken from the wrist joint during the prescribed motions must capture wrist JAEs. Some of the JAE signals most definitively related to joint pathology gathered in previous work come from Whittingslow et al.'s study on JAEs within a cadaver knee. In Whittingslow et al.'s study, observed JAEs did not exist in a knee before meniscus tear and meniscectomy. Thus, they could be directly attributed to changes within the articulating surfaces within the knee [9]. This work qualitatively assesses JAEs recorded from an additional volunteer who was afflicted with JIA as a child and has wrist acoustic emissions

which can be detected audibly. These recordings, as well as those from healthy volunteers, shown in Figure 2, closely resemble the grinding and clicking characteristic of JAEs from Whittingslow et al.'s study as well as the JAEs described in earlier studies [4], [9]–[11], [26] suggesting that this protocol successfully records JAEs from the wrist during both FE and rotation which are similar to those which have been able to provide salient joint health assessment in previous studies on the knee. JAEs from healthy volunteers are less frequent than JAEs from the volunteer with a history of JIA but are often periodic with the same period as the prescribed wrist motions (2 s), as is expected in JAE recordings from healthy volunteers [20], [57]. This shows that both exercises tested in this protocol are able to excite and record wrist JAEs.

JS divergence and intersession and intrasession ICC and CV are employed to assess the repeatability of the tested exercises to excite wrist JAEs [10,19]. The results indicate fair levels of intrasession and intersession repeatability in exciting JAEs with unweighted FE, and high levels of intrasession and intersession repeatability in recording JAEs from a wrist in rotation, with low variation between volunteers. The difference in repeatability in these exercises has moderate significance ($p < 0.05$ for intersession ICC and $p < 0.1$ for intrasession ICC, using two-sample t-test with Bonferroni correction), indicating rotation exercises more reliably create the dynamic interactions within the wrist joint which excite JAEs. Similar repeatability analysis using intrasession JS divergence (values closer to 0 indicate high levels of similarity) on the nine identified features extracted from the filtered acoustic signal confirms the high levels of repeatability also demonstrated by the ICCs. Both exercises show acceptable levels of signal strength with some variation between the healthy volunteers, but there is not a significantly better exercise for minimizing motion

artifacts ($p = 0.30$, using paired sample t-test with Bonferroni correction). However, SNR may be more dependent on microphone location due to motion artifacts. Thus, eliminating noisier locations would improve the overall performance of each exercise. In summary, both unweighted FE and rotation exercises can repeatably excite and record wrist JAEs with moderate signal strength, and the features of sounds which have performed well in knee joint health classification studies show high repeatability. Therefore, both unweighted wrist FE and rotation exercises are suitable for use in future clinical studies.

3.3.2 Evaluating Microphone Placement Locations Around the Wrist

It has been demonstrated that both wrist FE and rotation exercises consistently excite wrist JAEs which can be recorded by contact microphones placed on the surface of the skin around the wrist. However, some microphone placement locations have higher levels of noise due to motion artifacts. Quantifying this as an SNR value for each recording and summarizing by location yields the results displayed in Figure 3. Locations P1–P3 give the highest SNR values ($p < 0.001$, using two-sample t-test with Bonferroni correction), and locations D2 and M3 show moderately higher signal strength than the rest of the locations ($p < 0.001$, using two-sample t-test with Bonferroni correction). The standard deviation of SNRs among volunteers indicates some variability in noise levels at different locations among volunteers. Though this may alter which location produces the best signal quality for individual volunteers, the overall separation between proximal locations and all other locations indicates that the decreased skin motion relative to the underlying skeletal structure at these locations [46], [47] often minimizes motion artifacts within JAE recordings. Performing the same analysis to estimate SNR from a dataset of recordings from knee squats of healthy volunteers yields values similar to the SNR values gathered

around the wrist, indicating that recordings from the wrist have similar signal quality to those which have been correlated to joint health around the knee.

In the selected feature set, both within and between single-day recording sessions, intrasession and intersession ICC values demonstrate excellent repeatability in picking up JAEs at all locations except P1 and P2, which themselves have fair-to-good repeatability levels. Additionally, the standard deviation of ICC values across volunteers indicated low levels of variability between volunteers. Furthermore, the feature set shows moderate-to-low intrasession variability and moderate intersession variability. These repeatability findings compare favorably against a similar study from Kalo et al. on knee JAE repeatability which found intrasession ICCs of the median power frequency ranging from 0.85 to 0.95 at the tibia and 0.73 to 0.87 at the patella and intersession ICCs of the median power frequency ranging from 0.24 to 0.33 at the tibia and 0 to 0.82 at the patella [21]. This indicates the wrist recordings sense JAEs with similar or better repeatability levels than similar knee recordings in healthy volunteers at most locations. There is only enough separation to conclude location-specific reliability based on intrasession ICC with any statistical significance between the lowest performing location (P1) and the group of highest performing locations (D2 and M1–M3) ($p < 0.05$ for intrasession ICC, using two-sample t-test with Bonferroni correction), and separation decreases such that good separation ($p < 0.05$, using two-sample t-test with Bonferroni correction) is only present between the lowest (P1) and highest (M3) performing locations for intersession ICC. Additionally, the locations with highest repeatability levels also show the highest level of noise and motion artifact interference, which has been observed to inflate consistency measurements, further reducing the true separation between these measures across

locations. However, the degree of repeatability shown by the ICC (using measures which have been effective in knee JAE health classification [4], [9], [10], [17]) demonstrates any of these locations will record high quality JAEs [7] with similar consistency to recordings of knee JAEs from the top of the tibia and patella [21].

The combination of fair-to-high interrater repeatability demonstrated by ICC, intrarater repeatability demonstrated by JS divergence at all locations around the wrist, and the acceptable signal strength demonstrated with the SNR at locations P1–P3, D2, and M3 indicates that locations P1–P3, D2, and M3 are suitable for high quality repeatable wrist JAE recordings. The strong SNR values at locations P1–P3 have high separation over all other locations ($p < 0.001$, using two-sample t-test with Bonferroni correction), which had relatively weaker SNR scores. Additionally, the strongest signal strength demonstrated at location P1 shows high levels of separation from all other locations ($p < 0.001$, using two-sample t-test with Bonferroni correction). This reveals the best locations for minimizing artifact interference while still having fair repeatability are proximal to the wrist joint, and that location P1, which is 3 cm proximal to the wrist joint and centered between the radius and ulna on the dorsal side, is best for minimizing noise and motion artifact levels. On the other hand, locations P1 and P2 have the lowest levels of intersession and intrasession repeatability, which can be attributed to reduced proximity to the wrist joint and the fact that the soft tissue these locations rest upon will not transmit vibrations as well as the harder tissues of other locations [58], such as locations P3, D1, D2, and M1–M3, which are all clustered with high repeatability levels. The best balance of moderate-to-high signal strength and excellent repeatability of JAE recordings in healthy volunteers can be shown at locations P3, D2, and M3.

3.3.3 Limitations and Future Work

The volunteer sample size (n = 7) and the low-to-medium levels of variability between volunteers within these measurements means the sample of healthy volunteers may not be representative of a larger population with varied wrist joint pathologies. Future studies researching the effectiveness of quantifying wrist joint health using the locations described in this study must first perform qualitative assessments by looking at and listening to the audio signal to identify grinding and clicking sounds characteristic of JAEs to confirm the quality of wrist JAE recordings.

Locations P1–P3, D2, and M3 around the wrist have JAE recording quality and reliability levels during unweighted FE and rotation which compare well against similar measures around the knee during sit-to-stand and squats. These wrist locations and exercises can be employed as a framework for future studies aiming to show whether wrist JAEs demonstrate similar levels of diagnostic and treatment-tracking power for wrist injuries and degenerative diseases as previous studies centered around the knee presented [4], [7], [59], [9]–[13], [15]–[17]. This framework may also be used to create techniques for clinical use of wrist JAE recordings to facilitate quicker diagnosis of wrist joint injuries and chronic joint conditions and improved treatment progression monitoring. It may also allow for the development of wearable systems for at-home wrist joint health monitoring, which would provide clinicians with quantitative measurements to help assess patients' wrist joint health more frequently without the need for additional clinic visits, improving access to care, and therefore patient outcomes, while reducing the burden on the medical systems that treat such injuries and chronic joint conditions [59].

CHAPTER 4. DESIGN AND VALIDATION OF A WRIST WEARABLE SYSTEM FOR JAE MONITORING

The study detailed in CHAPTER 3 concludes that JAEs of the wrist can be produced repeatably during wrist FE and rotation exercises and mics may be placed on the skin at multiple specific locations around the wrist to reliably extract those JAE signals. These findings allow for the development of a wrist wearable system to monitor JAEs produced by the wrist in a clinical setting. Then, clinical research on the relevance of wrist JAEs to the wrist joint pathology will motivate development of a wrist wearable device for use in an at-home setting for remote joint health monitoring. Pediatric rheumatology practices could greatly benefit from such technology, as there is a shortage of physicians in this specialty. Patients who visit these specialists, such as those with JIA, often travels long distances for visits, accumulating large financial cost from missed school and work days, which is compounded by the need for multiple visits to follow up on treatment progression [3], [4]. Technological developments presented in this research facilitate telemedicine practices, which may improve the efficacy of pediatric rheumatology practices by expanding patients' access to care. This work aims to develop and validate a wrist wearable system for clinical monitoring of wrist JAEs in a pediatric patient population.

4.1 Wrist Wearable JAE Monitoring System Design

4.1.1 Electrical Design

The primary design constraint on a system for JAE extraction is that the electronics must sample microphones placed at multiple locations around the joint at a very high

frequency. Contact mics used in a wearable system should be highly sensitive, low profile, low noise, and have a wide band of frequencies where linear response is observed. Relatively inexpensive ($46 each) analog accelerometers with 10 mV/g sensitivity, 7.87x5.54x2.24 mm profile, and linear response up to 6 kHz (BU-23842-000, Knowles Electronics LLC., Itasca, IL USA) were selected to be used as contact mics in the wearable system. Custom PCB design and firmware were developed by Teague et al. to successfully accomplish high sample rate in four similar mics [25]. Therefore, much of the PCB design in this work utilizes the electrical hardware and firmware of the audio board developed by Teague et al. However, the current work has some distinct needs that Teague et al. did not have, so modifications were made to the PCB design and firmware. While the implementation of these modifications on the embedded system was performed by Göktuğ Cihan Özmen, a PhD student in the Inan Research Lab, conceptualization and overall design of the system was done in a collaborative manner.

The most prominent need in customizing the PCB designed by Teague et al. is miniaturization. The wrist is a smaller joint than the knee, and juvenile wrists further reduce the maximum size constraint of the PCB. The most important dimension of the PCB design and casing to limit is the radial-ulnar direction. The minimum expected age for children with JIA using at-home JAE monitoring is six years old, and the wrist circumference of a 5^{th} percentile six year old female is 10.70 cm [60]. Therefore, the maximum size of the wearable in the radial-ulnar direction should be 3 cm. The relative length of the forearm and lack of a set height constraint suggest dimensional constraints in the proximal-distal and dorsal-volar dimensions are less important. First, to minimize the size of the electronics in this design, three main adaptations are made. Electrical components are added to both

sides of the PCB rather than just one. Second, since board height is less important than width, the audio board is split into two smaller boards such that they can be connected by a robust, low-noise, and low cross talk capacitance board-to-board connector (Razor Beam, Samtec, New Albany, IN, USA). Third, the 500mAh Li-ion battery is replaced with a smaller 150mAh Li-ion battery.

An additional constraint in the customization of a PCB for a wrist wearable JAE monitoring device is it must synchronously record joint angle to analyze JAE signals on a cycle-by-cycle basis, as this has proven fruitful in joint health classification models using JAEs [4], [17]. Teague et al. use digital IMUs for joint angle measurement. Because mics are sampled at a very high frequency, ~46 kHz, a microcontroller was dedicated just for reading this high throughput data and writing it to a SD card as soon as possible without any data loss. Therefore, incorporating their IMU required additional hardware for microcontroller-to-sensors communication and sampling separate from the audio board [25]. Although this provides high quality orientation estimates with low noise, the primary drawback to incorporating the same sensors within a wrist wearable design is it would conflict with the goal of miniaturization. A flex-sensitive resistor, hereafter referred to as a flex sensor (FS2-L-055-103-ST, Spectra Symbol, Salt Lake City, UT, USA), is explored as an alternative. Flex sensors simply change resistance between two leads as they flex, reducing dedicated space allocation on the PCB, power consumption, and computational requirements. The trade-off to selecting this sensor is that unlike an IMU, polling the resistance of a flex sensor does not allow for extraction of precise joint angles. However, the benefits of the flex sensor outweigh this limitation because cycle extraction appears to be more important for subsequent JAE processing than exact joint angle, and the flex sensor

output should consistently allow for accurate cycle extraction. Additionally, exact joint angle extraction may still be obtained via calibration procedures which match resistance values with joint angles. The wearable device is designed using a resistor connected in series to a flex sensor, generating a simple voltage divider. The voltage drop on the flex sensor is sampled using an internal 12-bit ADC of the microcontroller. Since the goal is to obtain motion information (relatively low frequency), this voltage was sampled at 300 Hz and a moving average filter of 16 sample length is implemented on firmware. The data is then saved on a miniaturized secure digital card (microSD).

Another design requirement which requires special attention in the electronic design is the need for mic placement methods which minimize the introduction of motion artifacts and maximize the measured JAE signal strength and repeatability [22], [26]. One of the mic placement locations in this work is on the palm, so the mic may be held within a custom designed silicone grip, where the interface of the silicone of the grip and the user's skin minimizes slipping [61] and the user's grip strength provides a consistent backing force. To ensure consistent grip strength, the user must be provided feedback on the backing force of the mic in real time. A force sensitive resistor (FSR) (FSR® 402 Short, Interlink Electronics, Camarillo, CA, USA) is an inexpensive, flat, low-profile sensor which changes resistance across two leads as increasing force is applied to it. Using an FSR as a force sensor in this application minimizes the required space on the PCB, reduces power consumption, and eases mechanical design due to its low-profile. One primary drawback to FSRs is they do not provide high accuracy in force readings, so a simple resistance threshold was decided upon by comparing average output resistance against higher accuracy capacitive force sensors (CS8-10N, SingleTact, Los Angeles, CA, USA)

(capacitive force sensors are not used in the wearable design due to their vulnerability to damage via delamination) and configured into the firmware. FSR resistance is polled with the same methodology as the flex sensor. If the FSR reading indicates a good level of force is provided by the user, a green LED contained within a custom developed grip is illuminated to inform the user they are squeezing the grip with a proper level of force. Conversely, if the FSR indicates a poor amount of backing force is provided, a red LED within the grip is illuminated. The polled FSR data is also stored alongside the polled flex sensor data to help analyze motion artifacts created by insufficient grip strength and exclude cycles highly impacted by those artifacts from further analysis.

Once the primary sensing systems were selected, the adapted PCB layout was designed. The final PCB design has two boards, a mother and a daughter board, both 41 x 24mm, connected using board-to-board connectors. The daughter board sits closer to the wrist and mainly holds two aux ports to plug in mics (for modular system design), a custom designed analog front end with 21 dB gain and 32 Hz – 21.88 kHz bandwidth, an analog-to-digital converter (ADC) (ADAU1979, Analog Devices, Norwood, MA, USA), and solder pads to connect the FSR and flex sensor leads. The mother board sits atop the daughter board and has a battery connector, a microSD for data storage, a USB connector for data transfer and battery charging, a red switch to toggle system power, a white switch to toggle recording, and LEDs to indicate system power and recording status.

4.1.2 Mechanical Design and Fabrication

After the dimensions of the PCB layout were determined, the mechanical design was finalized as shown in Figure 4 (bill of materials in APPENDIX A. Bill of Materials.

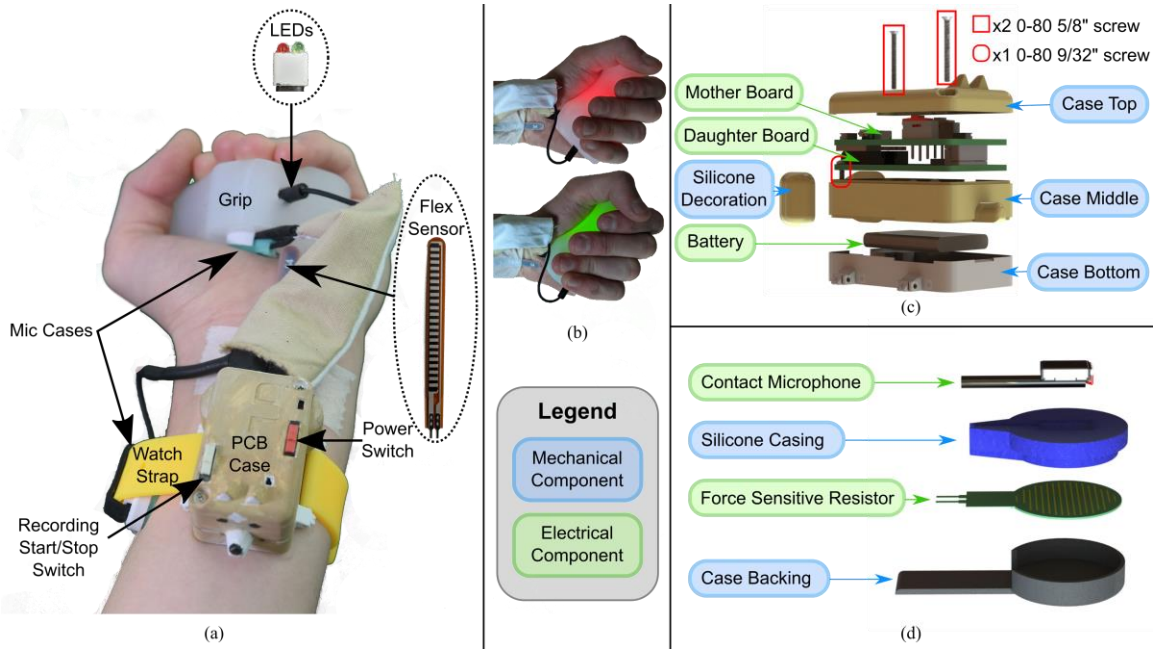

Figure 4: (a) Wrist wearable system as worn on the left wrist. Here, the force-feedback LEDs sit within the grip, which is grasped by the hand such that the distal mic, sitting within the mic case assembly and plugged into ch1 via wiring through the fabric sleeve to a straight audio jack, is pressed against the palm. The proximal mic is connected to ch4 via wiring to a right-angle audio jack, sits within a mic case underneath the adjustable watch strap, and is pressed against the radius by the tension of the watch strap. The PCB case, resembling a corgi dog, sits on the volar side of the forearm. The flex sensor protrudes distally from the PCB case and is taped flush against the forearm. (b) Demonstration of the red LED shining within the grip if the user's grip strength, sampled from the FSR, is insufficient and the green LED shining when the user's grip strength is sufficient. (c) Exploded view of the PCB case assembly. (d) Exploded view of the distal mic case assembly. The proximal mic case assembly is nearly identical, but lacks the FSR, and the backing lacks the rectangular platform beyond the cylinder and has a clip to attach to a watch strap loop.

The PCB is contained within a custom-designed 3D-printed Polylactic Acid (PLA) case. The assembly of the case, shown in Figure 4c, involves the PCB assembly placed between the top two layers of the case such that the switches extend through holes in the top layer for ease of access. A bottom layer holds the battery, flex sensor, and wiring from the PCB to the flex sensor, FSR, and external LEDs. The three case layers and the PCB are held together using three 0-80 machine screws screwed into heat-set inserts set within the

bottom layer of the PCB case. The full case assembly measures 44 mm in the proximal-distal dimension, 27 mm in the radial-ulnar direction, and 21.75 mm in the dorsal-volar (vertical) direction. Once assembled, only the power switch, recording switch, aux ports, and USB port are accessible by the user. The PCB case has “feet” on the bottom layer with small holes in the side to interface to the quick-release pins of commercial off-the-shelf 18 mm adjustable watch straps (18 mm Silicone Watch Band Strap with Quick Release Pins, GadgetWraps, Royal Oak, MI, USA).

In this work, two mics were placed at locations selected based on the signal strength and repeatability results demonstrated in 3.3.2 and the two different methods which a wearable system could use to affix the mics to the skin, one proximal location on the radius and one distal location centered between the first and second metacarpal bones on the palm (referred to as P3 and D2, respectively, in CHAPTER 3). Thus, if one mounting method performs well and the other does not, another high-performing location from CHAPTER 3 can be selected using the high performing mounting method for future design iterations. A mic casing (Figure 4d), inspired by the mic casings designed by Nevius [62] for applications in lung sound monitoring, was designed for improved JAE sensing without negatively impacting the transfer function of the mic within its region of performance (verified via experimentation in APPENDIX B. Mic Casing Characterization It uses a combination of a molded silicone case (Mold Max 40, Smooth-On, Easton, PA, USA) and a rigid 3D printed backing. Here, the proximal mic case has a clip on the back of the rigid backing to attach to the watch strap loops such that the case sits beneath the watch strap and the location of the mic case can be adjusted for any size wrist and either the left or right wrist. The high friction coefficient between the user’s skin and the silicone watchband and

mic case minimizes slipping [61], and the tension of the watchband across the mic case maintains a consistent backing force. The proximal mic utilizes a right-angle audio jack for improved wire management. The distal mic case is placed within a custom designed grip (Ecoflex 00-20, Smooth-On, Easton, PA, USA), where the high friction coefficient between the silicone grip and mic case and the user's skin minimizes slipping [61]. The FSR is placed between the silicone mic casing and the rigid backing so force applied to the mic is transmitted through the case, compressing the FSR. This provides a sensing modality for mic backing force to be used for grip strength feedback. The case backing is designed with an extended base so heat shrink tubing may fortify the FSR solder connections. LEDs are then placed within the grip as a visual medium for grip strength feedback (shown in Figure 4b). All wiring to the grip is contained within a sewn fabric sleeve for improved aesthetics. Lastly, the flex sensor extends from the lower level of the PCB case distally and is taped (Micropore Surgical Tape, 3M, Saint Paul, MN, USA) flush against the palmar side of the forearm such that wrist flexion bends the flex sensor.

4.1.3 Interaction with External Systems

The wrist wearable system design described in 4.1.1 and 0 can be used for untethered JAE audio signal extraction, motion tracking, and real time grip strength reinforcement. However, a computer is required to extract data from the wearable system's microSD for analysis. The data extraction program developed by Teague et al. [25] is used for this purpose.

Because a computer is required for data extraction, it may also be used for an additional purpose. The wearable system reads grip strength with an FSR and provides real

time feedback with LEDs to ensure the mic placed within the grip has sufficient backing force and records the FSR data. It also has a flex sensor to record joint motion. However, unlike the user input of grip strength, joint motion is not reinforced by the wearable. Two solutions have been developed to improve this user input. First, animations were developed so users could point their wrist at an animated character and follow the character's motion to prescribe a perfect 2 s periodic motion cycle. This system is meant for use with children, so multiple animated characters were developed to make the JAE recording more amusing. These animations, however, do not provide real time feedback to the user. In previous studies, motion feedback is provided by a trained researcher [4], [17], but this is not adequate within an at-home setting. Real time motion-reinforcement was developed utilizing color-tracking functionality in a MATLAB script, shown in Figure 5. By running this script alongside the guidance animations during the JAE recording sessions, the primary user input of wrist motion is reinforced near real time.

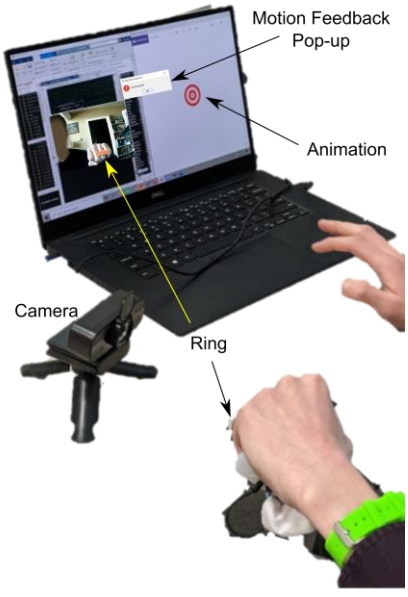

Figure 5: Real-time motion feedback system. The user wears a custom designed 3D printed PLA ring with a brightly colored green or yellow sticker on the hand which is

wearing the wearable device. A webcam is pointed at the user's hand, and the MATLAB script tracks the sticker's distinct color, highlights it with a red box, identifies the peak height of the red box in each motion cycle, takes the period between peaks, and creates a pop-up on the computer screen informing the user whether the previous wrist motion cycle was too fast or slow.

4.2 Design Validation Methods

4.2.1 Study Design and Ethics

The following study follows the Guidelines for Reporting Reliability and Agreement Studies (GRRAS) [51]. All human subjects research was conducted under approval by the Georgia Institute of Technology Institutional Review Board (#H20329). Volunteers provided written informed consent prior to participation in the study.

4.2.2 Participants

Six healthy college-aged volunteers (two male/four female, age 27.2 ± 1.5 years, mass 59.1 ± 9.6 kg, height 167.0 ± 12.7 cm, and wrist circumference 15.0 ± 0.9 cm) were recruited. Inclusion criteria for participation in this study dictated volunteers must have no history of major wrist injury or degenerative joint disease. Additionally, if volunteers had changes to wrist joint health between recording sessions, they would be excluded from the study. No volunteers met this exclusion criteria, so no such exclusions were made. Other factors which may affect wrist JAEs such as volunteers' daily medication usage, day-to-day wrist activity levels, and history of previous minor wrist injuries were not controlled.

4.2.3 Sensor Validation

The designed wrist wearable JAE monitoring device makes use of contact accelerometers for audio recording, a flex sensor for joint angle extraction, and an FSR for

grip strength reinforcement, all of which must be validated for their intended use. First, the flex sensor is validated by simultaneously recording the wrist performing FE, counter-clockwise (CCW) rotation, and clockwise (CW) rotation (10 cycles each, period 2 s) with the flex sensor of the wrist wearable and an IMU (BNO055, Adafruit Industries, New York, NY, USA) simultaneously. The same time segments of the raw recording output from both sensors are then plotted for qualitative comparisons, and the mean and standard deviation of peak-to-peak period is extracted for quantitative analysis.

Contact mic performance in recording JAEs must first be done qualitatively. An auditory inspection is performed by listening to the recording and comparing the sound of the JAEs to the JAEs recorded from the volunteer who had JIA as a child (see 3.1.2). Then, the audio signal is plotted in the time and frequency domain and visually compared to time and frequency domain plots from the volunteer who had JIA as a child as well as a benchtop recording from the same volunteer, wrist, placement location, and day as the wearable system recording.

The FSR is validated by plotting the data recorded from the polled FSR alongside the concurrent audio recording from the mic sitting atop the FSR on the distal mic location. Visual inspection should reveal high quality recordings when the FSR reads good backing force and increased prevalence of motion artifacts when poor backing force is applied.

4.2.4 Repeatability and Signal Strength Experiment Protocol

To assess the JAE recording repeatability and signal strength of the developed wrist wearable device and compare against the repeatability and signal strength of benchtop recordings, volunteers performed the following protocol on each of two days of study

participation, separated by less than a week. First, volunteers moved their wrists around for 20-30 s to remove artifacts from crepitus. Volunteers were then instructed to practice the prescribed FE, CCW rotation, and CW rotation exercises following the custom-developed character animations on a computer monitor. Two mics from the benchtop system described in 3.1.4 were then secured to the wrist at locations P3 and D2 shown in Figure 1. Wrist JAEs were recorded while the volunteers performed 10 exercise cycles, again following the provided animations, three times each for FE, CCW rotation, and CW rotation. This was repeated for the volunteer's other wrist. Then, the benchtop system was removed, and volunteers put on the wrist wearable JAE monitoring system as shown in Figure 4a. Wrist JAEs were recorded with the wearable system following the same procedure as described for the benchtop system.

4.2.5 Signal Extraction, Signal Processing, and Signal Strength Assessment

Benchtop signal extraction is performed exactly as described in 3.1.4 except with only the mic locations P3 (proximal) and D2 (distal), and the proximal mic was mounted on the skin with Kinesio tape instead of craft tape. Wearable system signal extraction is done by flipping the white switch proximally once the wearable system is worn as shown in Figure 4a to begin recording and flipping the white switch distally to end the recording.

Signal pre-processing is performed nearly exactly as described in 3.1.4 for both the wearable and benchtop systems. A smaller pass band (150 Hz–5.5 kHz) is used in the Kaiser-window bandpass filter because of the nonlinear behavior observed in the mics used by the wearable at frequencies higher than 6 kHz and their resonance around 10 kHz. The benchtop system continues to use an IMU for audio data segmentation, but the wearable

system uses flex sensor data. The first and last cycles of each JAE recording are discarded due to the relatively high prevalence of motion artifacts within those cycles, leaving 8 cycles per JAE recording for repeatability analysis. Signal strength analysis is performed exactly as described in 3.1.4 for both the wearable and benchtop systems.

4.2.6 Statistical Analysis

Statistical analysis is performed exactly as described in 3.1.5, except instead of using 10 cycles per recording, only 8 cycles per recording remain after the first and last cycles are discarded.

4.3 Validation Results

4.3.1 Sensor Validation Results

Concurrent raw flex sensor and IMU recordings of a wrist in motion used to validate flex sensor performance are shown in Figure 6. The mean and standard deviation of the peak-to-peak period of the IMU and flex sensor during 10 cycle recordings of FE, CCW rotation, and CW rotation are shown in Table 3. Audio recordings from the wrist wearable JAE recording device are visually compared to the benchtop system from the same volunteer, exercise, wrist, and placement location on the same day in Figure 7. A plot of wrist JAE recordings alongside recorded FSR data demonstrating the positive effect of proper grip strength on reducing artifact generation is shown in Figure 8.

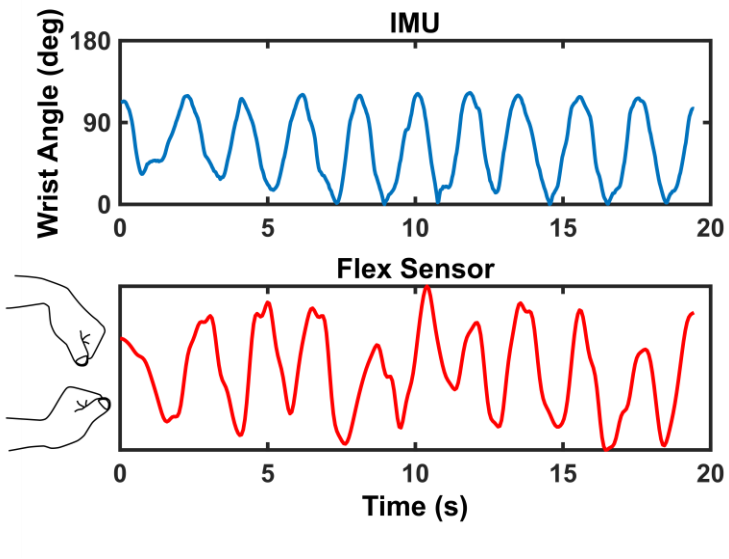

Figure 6: (Top) IMU recording of a wrist doing periodic (2 s) cycles of clockwise wrist rotation. (Bottom) Synchronous flex sensor recording.

Table 3. Peak-to-peak cycle period mean and standard deviation calculations from 10 exercise cycles of FE, CCW rotation and CW rotation, recorded synchronously with the flex sensor from the wrist wearable device and an IMU.

Exercise	Sensor	Cycle Period	
		Mean	Standard Deviation
Flexion-Extension	**IMU**	1.911	0.107
Flexion-Extension	**Flex Sensor**	1.890	0.224
CCW Rotation	**IMU**	1.852	0.653
CCW Rotation	**Flex Sensor**	1.862	0.148
CW Rotation	**IMU**	1.925	0.164
CW Rotation	**Flex Sensor**	1.943	0.358

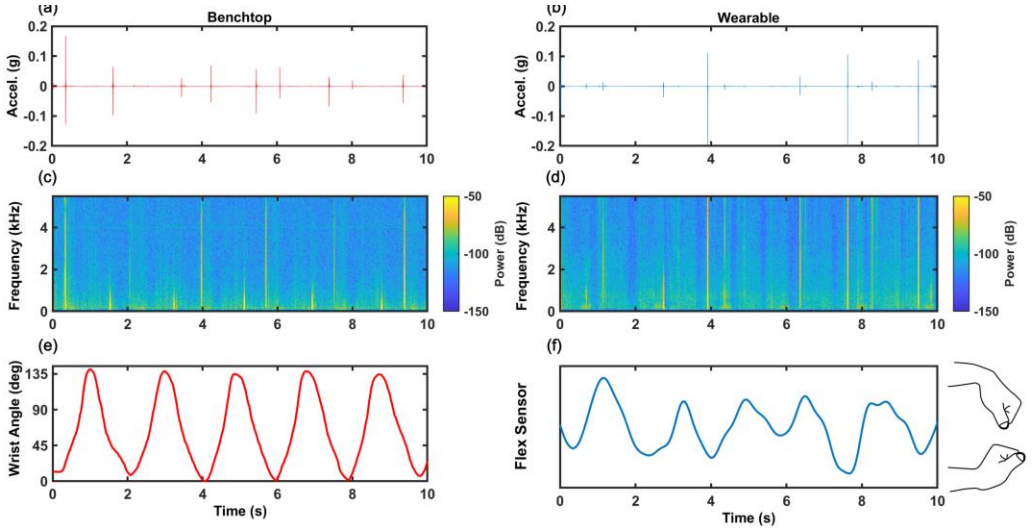

Figure 7: (a,c,e) Benchtop recording of JAEs from a volunteer performing wrist FE. (b,d,f) Wearable system recording of JAEs from wrist FE recorded from the same volunteer, wrist, mic location, and day. (a,b) Time domain of acoustic signal from the wrist. (c,d) Spectrogram of the acoustic signal displayed above it. (e,f) Motion data from the IMU and flex sensor recorded synchronously with the acoustic signal.

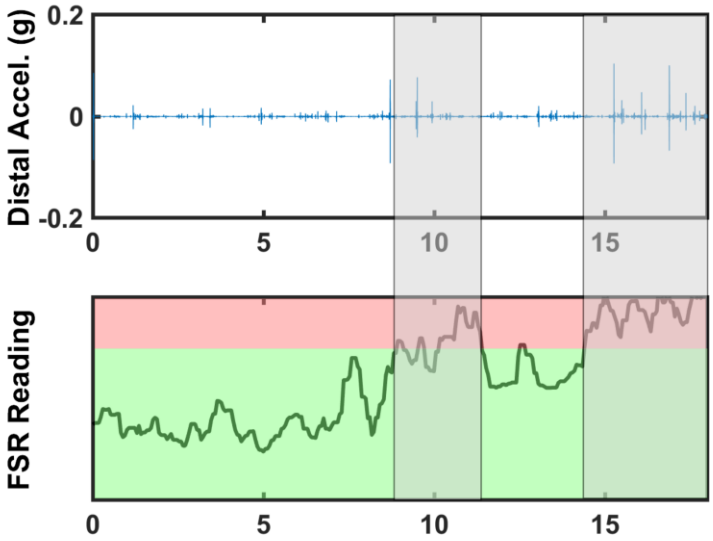

Figure 8: (Top) Distal mic audio JAE recording from a volunteer performing CCW wrist rotation. (bottom) Concurrent FSR recordings. The red region suggests poor grip strength, and FSR readings in this region cause a red LED to illuminate within the grip as shown in Figure 4. The green region represents proper grip strength, and FSR readings in this region cause a green LED to illuminate as shown in Figure 4.

4.3.2 Signal Strength

SNR distributions for both locations using each JAE measurement technique are displayed in Figure 9. At the proximal mic location, median SNR of the audio signal recorded by the benchtop JAE measurement system is 18.0 dB (95% CI of 16.8–19.2 dB) and has a standard deviation of 2.5 dB between subjects. The audio signal recorded by the wearable JAE measurement system at this location has a higher median SNR ($p < 0.001$, using two-sample t-test with Bonferroni correction) of 25.2 dB (95% CI of 24–26.3 dB) with a standard deviation of 3.1 between subjects. At the distal mic location, the median SNR of the JAE measurements recorded by the benchtop system is 16.6 dB (95% CI of 15.7–17.5 dB) with a standard deviation of 2.2 dB between subjects. The wearable JAE measurement system also has a higher SNR at this location ($p < 0.01$, using two-sample t-test with Bonferroni correction), as the median SNR is 18.1 dB (95% CI of 17.3–18.8 dB) with a standard deviation of 2.7 dB between subjects.

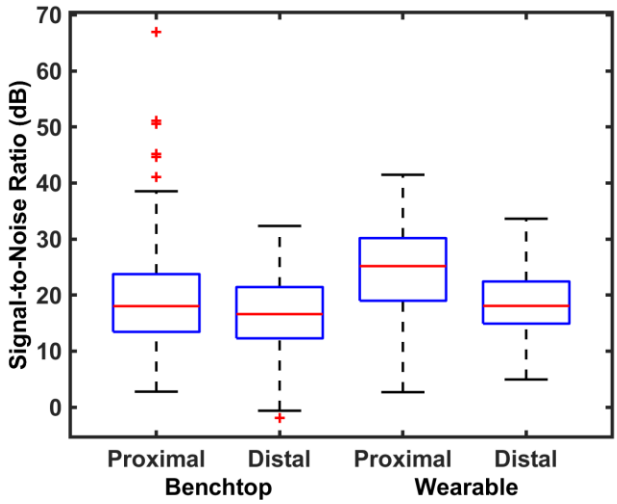

Figure 9: Box-and-whisker plot of SNR measurements of both the benchtop and wearable JAE measurement techniques at both mic placement locations after audio signals are filtered using a Kaiser-window bandpass filter with a passband of 150 Hz–5.5 kHz.

4.3.3 Reliability Measurements

Calculated measurements of interrater repeatability both within and between sessions using ICC (model 3,*k*) with a 95% confidence interval and inter-subject ICC standard deviation are displayed in Table 4. Table 4 also shows CV calculations. At the distal mic location, rater variability analysis using intrasession JS divergence of the nine selected features extracted from the filtered benchtop JAE acoustic signal gives a median JS divergence of 0.234 (95% CI of 0.228–0.241), whereas JAE recordings from the same location using the wearable system give a median JS divergence of 0.217 (95% CI of 0.210–0.223). At the proximal mic location, the median JS divergence of the benchtop JAE measurements is 0.225 (95% CI of 0.219–0.232), while the same location measured by the wearable system has a median JS divergence of 0.209 (95% CI of 0.202–0.215).

Table 4. Intersession and Intrasession repeatability values, including ICC with 95% CI upper and lower bounds, inter-subject ICC standard deviation, and CV.

		Benchtop		Wearable	
		Proximal	**Distal**	**Proximal**	**Distal**
Intrasession reliability	**ICC**	0.648	0.592	0.550	0.661
	Lower Bound	0.521	0.443	0.390	0.540
	Upper Bound	0.755	0.716	0.687	0.763
	Inter-subject ICC Std	0.013	0.108	0.124	0.030
	CV	0.136	0.164	0.132	0.122
Intersession reliability	**ICC**	0.669	0.593	0.554	0.707
	Lower Bound	0.495	0.374	0.319	0.554
	Upper Bound	0.806	0.762	0.738	0.828
	Inter-subject ICC Std	0.007	0.123	0.123	0.023
	CV	0.229	0.221	0.225	0.195

4.4 Discussion

4.4.1 Validation of Wrist Wearable JAE Monitoring System

Figure 6 shows the raw extracted signal of the flex sensor has a higher amount of noise than the IMU and is unable to extract precise joint angles. However, an IMU combines information from both an accelerometer and a gyroscope which is then processed using on-board signal processing techniques to refine its joint angle measurements. Signal processing techniques such as averaging and filtering can also be employed on the flex sensor signal to improve signal quality. Precise joint angles may never be extracted from the flex sensor signal because it simply outputs resistance changes during bending. However, cycle extraction is more important than specific joint angle extraction, and Table 3 shows that the flex sensor consistently allows for cycle extraction. Further, future work may develop calibration methods to extract precise joint angle from flex sensor measurements. Therefore, the flex sensor is suitable for wearable joint kinematic measurements.

The frequency band of JAE audio signals has been documented in low frequency ranges as a grinding sounds [26] up to high frequency (20kHz) components within the distinctive clicks [11]. The piezoelectric accelerometers employed as contact mics in the wearable system provide a linear response up to 6 kHz. This limits some of the information which can be extracted from JAE audio recordings, but the majority of JAE information is contained in frequencies lower than 5 kHz [22]. Therefore, a 5 kHz low pass filter can be employed to remove nonlinear behavior and retain most of the JAE information within JAE audio recordings. Qualitative auditory comparisons to wrist JAE recordings of a volunteer

who had JIA as a child and has audible joint sounds (shown in Figure 2) indicate the benchtop and wearable JAE monitoring systems can capture the grinding and clicking characteristic of JAEs. Figure 7 visually compares the wearable system to the validated benchtop system in both the time and frequency domains for the same volunteer, wrist, and location on the same day. Here, both systems demonstrate characteristic wide-band and short duration JAE events (clicks) which are periodic with the motion of the wrist, a characteristic trait of JAE recordings from healthy volunteers [20], [57]. The spectrogram shows similar frequency components in both systems. Unlike the wearable system, the benchtop system shows a resonance at both 2 kHz and 4 kHz. The source of this resonance has been traced to the mics used by the benchtop system, which require recalibration to remove the resonance behavior. This resonance is pervasive through all benchtop JAE recordings in this study. To ensure the resonances did not substantially affect the results of this study, signal strength and repeatability figures were reassessed with these frequencies filtered out. This change did not significantly change reported signal strength and repeatability results. Thus, the signal strength and repeatability figures of the wearable system may still accurately be compared to the same figures calculated from benchtop recordings. The combination of visual and auditory qualitative inspection reveals the wrist wearable system effectively captures JAEs from the selected distal and proximal locations. Additionally, spectrogram analysis shows the frequency content of the JAE recordings is not significantly altered by the presence of any resonances within the selected sensors or from the mechanical design. This shows the electronics and sensors of the developed wearable system have similar ability to capture JAEs as the established benchtop system. The noise floor of the system is also low enough not to cause issues in signal quality.

JAE recording quality is greatly impacted by artifact interference, and mic backing force is highly correlated to artifact production [26]. The implemented FSR within the distal mic case provides real time feedback to the user to reinforce proper grip strength. This has shown success, as users told to increase grip strength until they see the grip illuminate green have shown consistency in maintaining proper grip strength throughout JAE recordings. As a result, few recordings were identified which demonstrate how improper grip strength increased prevalence of motion artifacts. One recording which successfully demonstrates this effect shown in Figure 8. In this figure, time segments of improper grip strength are identified, and the corresponding distal mic JAE recording shows higher levels of artifact interference than the time segments with proper grip strength. This indicates the benefits to the FSR are twofold: real time feedback improves the quality of user-input, reducing prevalence of artifacts, and time segments which are more likely to contain artifacts can more easily be detected in later analysis.

JAE signals are low amplitude and are often inaudible to the human ear. Therefore, JAE measurement techniques must demonstrate the ability to capture JAE events and minimize the effects of noise and motion artifacts. The benchtop system this study uses as a baseline JAE capturing system has established its ability to capture JAEs with clinical relevance [4], [17], [52], [63]. A developed wearable JAE monitoring system must achieve similar signal strength within JAE recordings as the benchtop system to be considered for clinical use. Figure 9 shows the SNR of JAE measurements from the designed wearable system and the established benchtop system. The wearable system has demonstrably higher SNR at both locations ($p < 0.01$) with similar levels of subject-to-subject variability. Multiple factors may cause this difference. First, the benchtop system has long wires which

run from the DAQ to each mic. During motion cycles, these wires often brush against clothing, the floor, or even other wires, causing motion artifacts [64]. The wearable system does not employ these long wires, and employs techniques to improve backing force consistency, resulting in a reduction in mic slippage [26]. At the proximal location, this is accomplished by securing the mic between the watchband and the wrist, where the tension across the watchband applies a consistent moderate backing force when tightened so the watch is secure without cutting off circulation. The silicone of the mic case and watchband also have a high friction coefficient against skin, further preventing slippage [61]. At the distal location, the reduced artifact production may be attributed to two factors: the addition of a mic case, reducing mic movement within the grip, and the implementation of a real time grip strength feedback system, which noticeably reduces poor grip strength, thereby minimizing artifact creation, as is seen in Figure 8. These improvements improve JAE recording signal quality and improve system usability over the benchtop system, reducing the amount of training required by researchers, clinicians, and even study volunteers themselves, to record high quality JAEs.

The developed wrist wearable JAE monitoring device has shown to have the ability to record high quality JAEs. To be a viable product for use in a clinical setting, it must be able to capture JAEs with a high level of reliability. The interrater variability of JAE recordings in a healthy subject set is assessed both on a recording-to-recording (intrasession) and a day-to-day (intersession) basis with ICC (model 3,*k*), shown in Table 4. Both the benchtop and wearable systems show fair-to-good interrater reliability within a 95% CI at both locations, with no significant separation between the two systems ($p > 0.5$, using two-sample t-test with Bonferroni correction), indicating that when measured

with the selected raters, the benchtop system and wearable system will capture JAEs with similar levels of interrater reliability. The deviation in ICC calculations between volunteers shows the repeatability in recordings for both systems are similarly consistent across the sampled population. The variability within the calculated values of the selected raters within JAE recordings is assessed with JS divergence and CV. These measurements indicate that both the benchtop and wearable systems have moderate-to-low levels of variability within the calculated raters in JAE recordings. Although each CV and JS divergence calculation value is lower for the wearable system than the benchtop system (demonstrating lower intrarater variability), only JS divergence at the proximal location shows a moderate level of separation between the wearable and benchtop systems ($p < 0.1$, using two-sample t-test with Bonferroni correction). These results lead to the conclusion that JAE measurements from the designed wrist wearable system have similar levels of repeatability as the established benchtop system, where both systems have fair-to-good interrater reliability and moderate-to-low intrarater variability. When combined with the conclusions from qualitative assessment and SNR measurements, one may conclude the developed wrist wearable JAE monitoring system is able to capture JAEs from the wrist during FE, CCW rotation, and CW rotation exercises at locations around the wrist both proximal and distal to the wrist joint. Additionally, the JAE recordings from the wrist wearable JAE monitoring system demonstrate high signal strength relative to the established benchtop system with similarly acceptable levels of repeatability. Further, the wearable has been developed to have this high level of performance with improved usability and aesthetics. The combination of usability, aesthetics, and high performance make the developed wearable system suitable for use within a pediatric clinical setting.

4.4.2 Limitations and Future Work

The volunteer sample size (n = 6) and low-to-medium levels of variability between volunteers within the presented measurements means one cannot know if the sample of healthy volunteers in this study is representative of a larger population with varied wrist joint pathologies. Future studies researching the efficacy of quantifying wrist joint health using the developed wrist wearable JAE monitoring device must first perform qualitative assessments by looking at and listening to the audio signal to identify grinding and clicking sounds characteristic of JAEs to confirm the quality of wrist JAE recordings.

The results of this study demonstrate that the developed wrist wearable JAE monitoring system is suitable for use capturing JAEs within clinical studies investigating development of methods for quantifying wrist joint health. The wrist wearable device improves usability and aesthetics over the benchtop system, reduces the burden on clinical researchers for thorough training, and increases the appeal of study participation to potential subjects. The small form-factor and convenient design of this wearable system could also enable JAE measurements from other joints, such as the knee. For example, Whittingslow et al. recently demonstrated that JAEs measured from the knee using a benchtop system with two mics and a DAQ connected to a computer could be used to assess knee health of patients with JIA [4]. This wrist wearable system could be adapted to replace the benchtop system used in that study and enable knee health monitoring at home. The current design of the wrist wearable JAE monitoring system is simple enough to use that "super-users" could be trained to use the system without any assistance from a clinician, making it suitable for at-home joint health monitoring if the device is returned to the clinic for the clinician to download the JAE recordings onto a computer to be processed later.

If future studies indicate JAEs from the wrist may reliably track treatment progression, a wearable JAE monitoring device could be converted into a product for at-home wrist joint health monitoring. However, the current system is not yet suitable for widespread at-home use, especially in a juvenile population. First, the aesthetics of the device would require refinement. Specifically, wires outside of the confines of a custom-developed grip and the wrist-worn PCB case should be limited. This can be accomplished in future iterations with a two-device design and Bluetooth communication between devices, where the master PCB is worn on the wrist, and the slave PCB is contained within the grip. Additionally, the flex sensor taped to the forearm can be eliminated if a mic distal to the wrist joint could be low pass filtered with a cutoff frequency marginally higher than the prescribed frequency of wrist motion. Currently, the analog front-end (AFE) designed by Teague et al. for the analog accelerometers has an inherent high pass filter (f_c = 32 Hz), limiting this ability. As recent studies show most of the information in JAEs is below 5 kHz, a move to lower bandwidth digital accelerometers in future iterations would allow for this change while also eliminating the space on the PCB required for the AFE, improving miniaturization. Employing digital accelerometers would also reduce the processing load on the microcontroller so the microcontroller would be able to handle communication to IMUs for high accuracy joint angle measurement, if desired. Another key weakness in the move to at-home monitoring is that the device requires a computer running the program developed by Teague et al. [25] to download data off of the device. Future iterations should allow Bluetooth communication to a computer while the device is not in use so data can be remotely sent to a physician via a secure pathway (such as a patient portal within an EMR). A computer with MATLAB installed is also required within the current iteration for real

time motion reinforcement, reducing broad usability. Because Bluetooth communication with the computer is the preferred method of data transfer from the wearable to the computer in future iterations, motion capture data could be sent real time via Bluetooth to be processed by a custom-developed application for real time motion reinforcement. Additionally, because digital accelerometers reduce processing load on the micro-controller, digital load cells could be included in the system to replace FSRs. This data may also be sent via Bluetooth so both motion reinforcement and grip strength reinforcement can be done real time from a computer application. This application may also be designed specifically for use by children to improve usability within a pediatric population.

CHAPTER 5. CONCLUSION

This dissertation has presented research with two primary aims. First, methods of knee JAE extraction were studied. Based on established methods of producing, recording, and analyzing meaningful JAEs from the knee, a framework to produce and record wrist JAEs was developed and validated to expand research in JAEs to the wrist joint. Second, using the developed framework for producing and recording JAEs from the wrist, a wrist wearable JAE monitoring system was designed, fabricated, and validated for use in pediatric clinical studies.

In the pursuit of these aims, multiple conclusions were made. First, to the best available knowledge, it was found passive JAEs can be produced from a wrist performing cyclical FE and rotation exercises, and these JAEs can be reliably recorded using a framework which employs highly sensitive wide-band uniaxial accelerometers secured on the surface of the skin. Once the wrist JAE audio is recorded alongside simultaneous wrist joint angle measurement recordings, these recordings could be used in research for wrist joint health quantification. Second, to the best available knowledge, the first ever wrist wearable JAE measurement system was developed to facilitate wrist JAE extraction in clinical and at-home settings. In validation, it was found that this system successfully captures wrist JAE audio and simultaneous wrist joint motion. When compared to a previously validated benchtop system, the wearable system records JAEs with higher signal strength relative to the noise and artifacts produced during recordings and demonstrates fair-to-good levels of repeatability and reliability, the same level of repeatability and reliability found in recordings using the established benchtop system.

There is a clear path for future work to build upon the work described in this thesis. First, clinical research should utilize the developed framework for wrist JAE recording to conduct studies investigating whether wrist JAEs may be used as a quantitative measure to aid in wrist joint health assessment, as has been done in studies focused on JAEs of the knee. Such studies may either employ a JAE capturing system based on the framework created within the first aim of this work, or they may employ the wrist wearable system developed and validated in this work's second aim. If the clinical research concludes that wrist JAEs can be used for wrist joint health quantification, the developed wearable system may be revised to be better suited for at-home use as a tool for clinicians to quantitatively assess wrist joint health remotely, reducing pressure on health systems and greatly benefitting a patient population which currently relies on invasive, qualitative, or expensive health assessment methods in repeated clinic visits.

APPENDIX A. BILL OF MATERIALS

Table 5. Bill of materials required for assembly of the designed wrist wearable JAE monitoring device. The total price per assembly is $808.57 when materials are purchased for full assembly of eight wearable devices.

Function	Component	Price per assembly
Electronics	Audio board - mother board	$ 315.13
Electronics	Audio board - daughter board	$ 321.32
Power supply	Lithium Battery 3.7V 150mAh	$ 5.95
Data Storage	Samsung 32 GB EVO UHS-I microSDHC	$ 7.49
Motion tracking	Spectra Symbol FLEX SENSOR 10K OHM	$ 21.00
Mic contact force sensor	Interlink Electronics FSR® 402	$ 9.90
Contact microphone qty 2	Knowles BU-23842-000-ND	$ 104.46
Grip	Custom molded EcoFlex 00-30 grip	$ 2.00
PCB housing	PLA 3D print	$ 0.05
Fastening qty 1	0-80 9/32" screw	$ 0.06
Fastening qty 2	0-80 5/8" screw	$ 0.22
Fastening qty 3	0-80 heat set insert	$ 0.37
Mic Case	Printed backing and molded EcoFlex 00-30 case	$ 0.06
Strap to wrist	Watch Strap	$ 13.95
Adjust Mic Placement	Watch Strap loop	$ 0.87
Audio Jack	Audio Jack straight	$ 1.68
Audio Jack	Audio Jack right angle	$ 2.02
Flex sensor and wire encasement	Fabric Sleeve	$ 2.04
Decoration	Paints - tan, white, and black	$ 1.86

APPENDIX B. MIC CASING CHARACTERIZATION

Mic casings are designed to improve JAE sensing, protect the contact mics, and improve the method of attachment to the skin surface, reducing the likelihood of artifact introduction [26] and improving the sensitivity of mics to frequency ranges important to JAE analysis [22]. The mic cases designed in this work are based on a design by Nevius for lung sound monitoring [62], but differing requirements in this work have necessitated modifications which have led to two different mic casings (described in 4.1.2): one distal and one proximal. These casings are designed to improve JAE sensing, so it is necessary to ensure they do not negatively affect the sensitivity of the mic within the frequency range used in the analysis of JAEs recorded by the developed wrist wearable JAE monitoring device (150 Hz – 5.5 kHz). To quantify the impact of these casings on the sensitivity, they were subjected to shaker vibration testing using the setup shown in Figure 10.

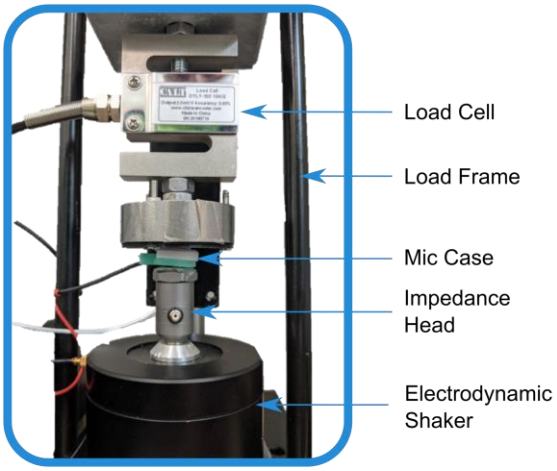

Figure 10: Testing setup for the mic case shaker tests.

In this test, a custom MATLAB script generates a sine wave excitation sweep signal from 100 Hz – 10 kHz over the course of 50 seconds. This signal is sent to the output channel of a DAQ (USB-4431, National Instruments, Austin, TX, USA), then through a

power amplifier (B&K Type 2718 Power Amplifier, Brüel & Kjær, Nærum, Denmark) to a shaker (B&K Type 4810 Mini Shaker, Brüel & Kjær, Nærum, Denmark) for excitation of the mic cases. An in-line reference impedance head (B&K Type 8001 Impedance Head, Brüel & Kjær, Nærum, Denmark) is powered and amplified by a charge amplifier (Type 5011, Kistler, Winterthur, Switzerland) to measure the input acceleration via an input channel of the DAQ at a sampling rate of 50 kHz. The mic casing is mounted on top of the impedance head, and a load frame applies a consistent 1N force to the mic case as measured by a load cell (DYLY-103, CALT, Shanghai, China) connected via an in-line amplifier (UV Series Inline Amplifier, Honeywell, Charlotte, NC, USA) to an input channel of the DAQ. A low-friction tape (Ultra-Low-Friction Tape, McMaster-Carr, Elmhurst, IL, USA) in tension is pressed across the back of the mic case for uniform backing force. The output is measured by the mic contained within the mic case and connected to an input channel on the DAQ.

Input-output coherence of these measurements is very high (>0.99) in the tested band of frequencies (100 Hz – 10 kHz), suggesting vibration measurements are reliable. The transfer functions of the mic with no casing (baseline), mic with proximal mic casing, and mic with distal mic casing are shown in Figure 11. Results show the developed mic cases introduce no resonance behavior to the system not already present in the mic, and there is minimal difference in transfer functions with or without the mic case before the response begins to be nonlinear (~ 6 kHz). Additionally, higher frequencies are filtered out in JAE analysis because of known nonlinear mic sensitivity. Therefore, the designed mic casings do not negatively alter the transfer function of the mic within the frequency band used in the analysis of JAEs recorded by the developed wrist wearable and may therefore

be used for high quality JAE measurement within the developed wrist wearable JAE measurement system.

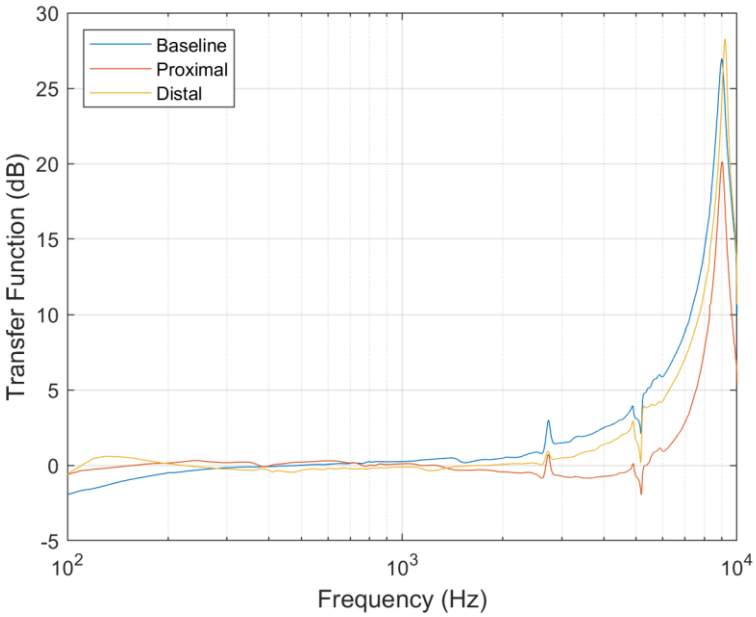

Figure 11: Transfer function measurement results of mic with no casing (baseline), mic with proximal mic casing, and mic with distal mic casing.

REFERENCES

[1] A. D. Woolf and K. Åkesson, "Understanding the burden of musculoskeletal conditions," *Br. Med. J.*, vol. 322, no. 7294, pp. 1079–1080, 2001, doi: 10.1136/bmj.322.7294.1079.

[2] O. T. Inan *et al.*, "Wearable knee health system employing novel physiological biomarkers," *J. Appl. Physiol.*, vol. 124, no. 3, pp. 537–547, 2018, doi: 10.1152/japplphysiol.00366.2017.

[3] C. L. Deal *et al.*, "The United States rheumatology workforce: Supply and demand, 2005-2025," *Arthritis Rheum.*, vol. 56, no. 3, pp. 722–729, 2007, doi: 10.1002/art.22437.

[4] D. C. Whittingslow *et al.*, "Knee Acoustic Emissions as a digital biomarker of disease status in Juvenile Idiopathic Arthritis," *Front. Digit. Heal.*, 2020, doi: 10.3389/fdgth.2020.571839.

[5] W. E. Blodgett, "Auscultation of the knee joint," *Bost. Med. Surg. J.*, vol. 146, no. 3, pp. 63–66, 1902, doi: 10.1056/nejm190201161460304.

[6] S. Hersek *et al.*, "Wearable vector electrical bioimpedance system to assess knee joint health," *IEEE Trans. Biomed. Eng.*, vol. 64, no. 10, pp. 2353–2360, 2017, doi: 10.1109/TBME.2016.2641958.

[7] S. Hersek *et al.*, "Acoustical emission analysis by unsupervised graph mining: A novel biomarker of knee health status," *IEEE Trans. Biomed. Eng.*, vol. 65, no. 6, pp. 1291–1300, 2018, doi: 10.1109/TBME.2017.2743562.

[8] C. Teague *et al.*, "Novel approaches to measure acoustic emissions as biomarkers for joint health assessment," in *2015 IEEE 12th International Conference on Wearable and Implantable Body Sensor Networks, BSN 2015*, 2015, pp. 1–6, doi: 10.1109/BSN.2015.7299389.

[9] D. C. Whittingslow, H. K. Jeong, V. G. Ganti, N. J. Kirkpatrick, G. F. Kogler, and O. T. Inan, "Acoustic emissions as a non-invasive biomarker of the structural health of the knee," *Ann. Biomed. Eng.*, vol. 48, pp. 225–235, 2020, doi: 10.1007/s10439-019-02333-x.

[10] B. Semiz, S. Hersek, D. C. Whittingslow, L. A. Ponder, S. Prahalad, and O. T. Inan, "Using knee acoustical emissions for sensing joint health in patients with Juvenile Idiopathic Arthritis: A Pilot Study," *IEEE Sens. J.*, vol. 18, no. 22, pp. 9128–9136, 2018, doi: 10.1109/JSEN.2018.2869990.

[11] B. Semiz, S. Hersek, D. C. Whittingslow, L. Ponder, S. Prahalad, and O. T. Inan, "Change point detection in knee acoustic emissions using the teager operator: A

preliminary study in patients with juvenile idiopathic arthritis," in *2019 IEEE EMBS International Conference on Biomedical and Health Informatics, BHI 2019 - Proceedings*, 2019, pp. 1–4, doi: 10.1109/BHI.2019.8834607.

[12] C. B. Frank, R. M. Rangayyan, and G. D. Bell, "Analysis of knee joint sound signals for non-invasive diagnosis of cartilage pathology," *IEEE Eng. Med. Biol. Mag.*, vol. 9, no. 1, pp. 65–68, 1990, doi: 10.1109/51.62910.

[13] N. Befrui *et al.*, "Vibroarthrography for early detection of knee osteoarthritis using normalized frequency features," *Med. Biol. Eng. Comput.*, vol. 56, pp. 1499–1514, 2018, doi: 10.1007/s11517-018-1785-4.

[14] T. I. Khan, M. Kusumoto, Y. Nakamura, S. Ide, and T. Yoshimura, "Acoustic emission technique as an adaptive biomarker in integrity analysis of knee joint," in *Journal of Physics: Conference Series*, 2018, doi: 10.1088/1742-6596/1075/1/012020.

[15] S. Ota *et al.*, "Preliminary study of optimal measurement location on vibroarthrography for classification of patients with knee osteoarthritis," *J. Phys. Ther. Sci.*, vol. 28, no. 10, pp. 2904–2908, 2016, doi: 10.1589/jpts.28.2904.

[16] P. Madeleine, R. E. Andersen, J. B. Larsen, L. Arendt-Nielsen, and A. Samani, "Wireless multichannel vibroarthrographic recordings for the assessment of knee osteoarthritis during three activities of daily living," *Clin. Biomech.*, vol. 72, pp. 16–23, 2020, doi: 10.1016/j.clinbiomech.2019.11.015.

[17] S. Gharehbaghi, D. C. Whittingslow, L. A. Ponder, S. Prahalad, and O. T. Inan, "Acoustic emissions from loaded and unloaded knees to assess joint health in patients with Juvenile Idiopathic Arthritis," unpublished.

[18] H. K. Jeong, M. B. Pouyan, D. C. Whittingslow, V. Ganti, and O. T. Inan, "Quantifying the effects of increasing mechanical stress on knee acoustical emissions using unsupervised graph mining," *IEEE Trans. Neural Syst. Rehabil. Eng.*, vol. 26, no. 3, pp. 594–601, 2018, doi: 10.1109/TNSRE.2018.2800702.

[19] *Treatment Guide: Knee Pain*. (2018). Cleveland Clinic. [Online]. Available: https://my.clevelandclinic.org/ccf/media/files/ortho/knee_pain_guide

[20] C. N. Teague *et al.*, "Novel methods for sensing acoustical emissions from the knee for wearable joint health assessment," *IEEE Trans. Biomed. Eng.*, vol. 63, no. 8, pp. 1581–1590, 2016, doi: 10.1109/TBME.2016.2543226.

[21] K. Kalo, D. Niederer, R. Sus, K. Sohrabi, V. Groß, and L. Vogt, "Reliability of vibroarthrography to assess knee joint sounds in motion," *Sensors (Switzerland)*, vol. 20, no. 7, 2020, doi: 10.3390/s20071998.

[22] G. C. Ozmen, M. Safaei, L. Lan, and O. T. Inan, "A novel accelerometer mounting method for sensing performance improvement in acoustic measurements from the

knee," *J. Vib. Acoust.*, vol. 143, no. 3, 2021, doi: 10.1115/1.4048554.

[23] K. Kalo *et al.*, "Validity of and recommendations for knee joint acoustic assessments during different movement conditions," *J. Biomech.*, vol. 109, p. 109939, 2020, doi: 10.1016/j.jbiomech.2020.109939.

[24] D. M. Hochman, S. Gharehbaghi, D. C. Whittingslow, and O. T. Inan, "A pilot study to assess the reliability of sensing joint acoustic emissions of the wrist," *Sensors (Switzerland)*, vol. 20, no. 15, pp. 1–13, 2020, doi: 10.3390/s20154240.

[25] C. N. Teague *et al.*, "A wearable , multimodal sensing system to monitor knee joint health," *IEEE Sens. J.*, vol. 20, no. 18, pp. 10323–10334, 2020.

[26] N. B. Bolus, H. K. Jeong, D. C. Whittingslow, and O. T. Inan, "A glove-based form factor for collecting joint acoustic emissions: design and validation," *Sensors (Switzerland)*, vol. 19, no. 12, pp. 1–11, 2019, doi: 10.3390/s19122683.

[27] A. C. Rettig, "Epidemiology of hand and wrist injuries in sports," *Clin. Sports Med.*, vol. 17, no. 3, pp. 401–406, Jul. 1998, doi: 10.1016/S0278-5919(05)70092-2.

[28] L. S. Robinson, T. Brown, and L. O'Brien, "Capturing the costs of acute hand and wrist injuries: Lessons learnt from a prospective longitudinal burden of injury study," *Hand Ther.*, vol. 25, no. 4, 2020, doi: 10.1177/1758998320952815.

[29] H. Akhondi and S. Panginikkod, "Wrist arthritis," *Open Access Publ. by UMMS Authors*, 2018, [Online]. Available: https://escholarship.umassmed.edu/oapubs/3646.

[30] A. F. Hoeksma, W. G. Zinger, M. A. van Rossum, K. M. Dolman, J. Dekker, and L. D. Roorda, "THU0297 High prevalence of hand and wrist impairments in juvenile idiopathic arthritis (JIA)," *Ann. Rheum. Dis.*, vol. 71, p. 256, 2013, doi: 10.1136/annrheumdis-2012-eular.2262.

[31] C. E. De Putter, R. W. Selles, S. Polinder, M. J. M. Panneman, S. E. R. Hovius, and E. F. Van Beeck, "Economic impact of hand and wrist injuries: Health-care costs and productivity costs in a population-based study," *J. Bone Jt. Surg. - Ser. A*, vol. 94, no. 9, p. e56, 2012, doi: 10.2106/JBJS.K.00561.

[32] R. Shehab and M. H. Mirabelli, "Evaluation and diagnosis of wrist pain: A case-based approach," *Am. Fam. Physician*, vol. 87, no. 8, pp. 568–573, Apr. 2013, Accessed: Feb. 08, 2021. [Online]. Available: www.aafp.org/afp.

[33] G. I. Bain, J. Munt, and P. C. Turner, "New advances in wrist arthroscopy," *Arthrosc. - J. Arthrosc. Relat. Surg.*, vol. 24, no. 3, pp. 355–367, 2008, doi: 10.1016/j.arthro.2007.11.002.

[34] D. Fuller *et al.*, "Reliability and validity of commercially available wearable devices for measuring steps, energy expenditure, and heart rate: Systematic review," *JMIR*

mHealth uHealth, vol. 8, no. 9, 2020, doi: 10.2196/18694.

[35] K. Kaewkannate and S. Kim, "A comparison of wearable fitness devices," *BMC Public Health*, vol. 16, no. 433, 2016, doi: 10.1186/s12889-016-3059-0.

[36] M. Ghamari, "A review on wearable photoplethysmography sensors and their potential future applications in health care," *Int. J. Biosens. Bioelectron.*, vol. 4, no. 4, 2018, doi: 10.15406/ijbsbe.2018.04.00125.

[37] S. R. Steinhubl *et al.*, "Effect of a home-based wearable continuous ECG monitoring patch on detection of undiagnosed atrial fibrillation: The mSToPS randomized clinical trial," *JAMA - J. Am. Med. Assoc.*, vol. 320, no. 2, pp. 146–155, 2018, doi: 10.1001/jama.2018.8102.

[38] F. Axisa, P. M. Schmitt, C. Gehin, G. Delhomme, E. McAdams, and A. Dittmar, "Flexible technologies and smart clothing for citizen medicine, home healthcare, and disease prevention," *IEEE Trans. Inf. Technol. Biomed.*, vol. 9, no. 3, pp. 325–336, 2005, doi: 10.1109/TITB.2005.854505.

[39] A. Kamiŝalić, I. Fister, M. Turkanović, and S. Karakatiĉ, "Sensors and functionalities of non-invasive wrist-wearable devices: A review," *Sensors (Switzerland)*, vol. 18, no. 6, 2018, doi: 10.3390/s18061714.

[40] A. Nemcova *et al.*, "Monitoring of heart rate, blood oxygen saturation, and blood pressure using a smartphone," *Biomed. Signal Process. Control*, vol. 59, 2020, doi: 10.1016/j.bspc.2020.101928.

[41] P. Mosconi, S. Radrezza, E. Lettieri, and E. Santoro, "Use of health apps and wearable devices: Survey among Italian associations for patient advocacy," *JMIR mHealth uHealth*, vol. 7, no. 1, p. e10242, 2019, doi: 10.2196/10242.

[42] H. K. Jeong, D. Whittingslow, and O. T. Inan, "b -Value: A potential biomarker for assessing knee-joint health using acoustical emission sensing," *IEEE Sensors Lett.*, vol. 18, no. 22, pp. 9128–9136, 2018, doi: 10.1109/lsens.2018.2871981.

[43] S. K. Charles and N. Hogan, "Dynamics of wrist rotations," *J. Biomech.*, vol. 44, no. 4, pp. 614–621, 2011, doi: 10.1016/j.jbiomech.2010.11.016.

[44] P. Coutsoukis, "Surface markings of the upper extremities," 1995. https://theodora.com/anatomy/surface_anatomy_of_the_upper_extremity.html.

[45] A. G. Fam, G. V. Lawry, and H. J. Kreder, *Musculoskeletal Examination and Joint Injection Techniques*. 2006.

[46] J. H. Ryu, N. Miyata, M. Kouchi, M. Mochimaru, and K. H. Lee, "Analysis of skin movement with respect to flexional bone motion using MR images of a hand," *J. Biomech.*, vol. 39, no. 5, pp. 844–852, 2006, doi: 10.1016/j.jbiomech.2005.02.001.

[47] R. Richard, J. Ford, S. F. Miller, and M. Staley, “Photographic measurement of volar forearm skin movement with wrist extension: The influence of elbow position,” *J. Burn Care Rehabil.*, vol. 15, no. 1, pp. 58–61, 1994, doi: 10.1097/00004630-199401000-00011.

[48] H. Toreyin, S. Hersek, C. N. Teague, and O. T. Inan, “A proof-of-concept system to analyze joint sounds in real time for knee Health assessment in uncontrolled settings,” *IEEE Sens. J.*, vol. 19, no. 9, pp. 2892–2893, 2016, doi: 10.1109/JSEN.2016.2522964.

[49] A. Mosenia, S. Sur-Kolay, A. Raghunathan, and N. K. Jha, “Wearable medical sensor-based system design: A survey,” *IEEE Trans. Multi-Scale Comput. Syst.*, vol. 3, no. 2, pp. 124–138, 2017, doi: 10.1109/TMSCS.2017.2675888.

[50] F. Gemperle, C. Kasabach, J. Stivoric, M. Bauer, and R. Martin, “Design for wearability,” in *International Symposium on Wearable Computers, Digest of Papers*, 1998, pp. 116–122, doi: 10.1109/ISWC.1998.729537.

[51] J. Kottner *et al.*, “Guidelines for Reporting Reliability and Agreement Studies (GRRAS) were proposed,” *Int. J. Nurs. Stud.*, vol. 48, no. 6, pp. 661–671, 2011, doi: 10.1016/j.ijnurstu.2011.01.016.

[52] G. C. Ozmen *et al.*, “Detection of meniscal tear effects on tibial vibration using passive knee sound measurements,” *IEEE Trans. Biomed. Eng.*, 2021, doi: 10.1109/TBME.2020.3048930.

[53] T. K. Koo and M. Y. Li, “A guideline of selecting and reporting intraclass correlation coefficients for reliability research,” *J. Chiropr. Med.*, vol. 15, no. 2, pp. 155–163, 2016, doi: 10.1016/j.jcm.2016.02.012.

[54] J. L. Fleiss, *The Design and Analysis of Clinical Experiments*. 1999.

[55] F. Pérez-Cruz, “Kullback-leibler divergence estimation of continuous distributions,” in *IEEE International Symposium on Information Theory - Proceedings*, 2008, pp. 1666–1670, doi: 10.1109/ISIT.2008.4595271.

[56] B. Fuglede and F. Topsøe, “Jensen-Shannon divergence and Hilbert space embedding,” in *IEEE International Symposium on Information Theory - Proceedings*, 2004, p. 31, doi: 10.1109/isit.2004.1365067.

[57] A. D. Wiens, S. Prahalad, and O. T. Inan, “VibroCV: A computer vision-based vibroarthrography platform with possible application to Juvenile idiopathic arthritis,” in *Proceedings of the Annual International Conference of the IEEE Engineering in Medicine and Biology Society, EMBS*, 2016, pp. 4431–4434, doi: 10.1109/EMBC.2016.7591710.

[58] M. Safaei, N. B. Bolus, A. Erturk, and O. T. Inan, “Vibration characterization of the human knee joint in audible frequencies,” *Sensors (Switzerland)*, vol. 20, no. 15, pp.

1–13, 2020, doi: 10.3390/s20154138.

[59] Y. Athavale and S. Krishnan, “A telehealth system framework for assessing knee-joint conditions using vibroarthrographic signals,” *Biomed. Signal Process. Control*, vol. 55, p. 101580, 2020, doi: 10.1016/j.bspc.2019.101580.

[60] A. Öztürk, B. Çiçek, M. M. Mazıcıoğlu, G. Zararsız, and S. Kurtoğlu, “Wrist circumference and frame size percentiles in 6-17-year-old Turkish children and adolescents in Kayseri,” *JCRPE J. Clin. Res. Pediatr. Endocrinol.*, vol. 9, no. 4, pp. 329–336, 2017, doi: 10.4274/jcrpe.4265.

[61] M. Zhang and A. F. T. Mak, “In vivo friction properties of human skin,” *Prosthet. Orthot. Int.*, vol. 23, no. 2, pp. 135–141, 1999, doi: 10.3109/03093649909071625.

[62] B. Nevius, “The mechanical design and optimization of a wearable multimodal health sensing system,” M.S. thesis, Woodruff School of Mechanical Engineering, Georgia Institute of Technology, Atlanta, 2020.

[63] D. C. Whittingslow, L. Orlandic, T. Gergely, S. Prahalad, O. T. Inan, and S. Abramowicz, “Acoustic emissions of the temporomandibular joint in children: Proof of Concept,” *Front. Oral Maxillofac. Med.*, no. In Press, pp. 1–8, 2020, doi: 10.21037/fomm-20-10.

[64] G. C. Ozmen *et al.*, “An interpretable experimental data augmentation method to improve knee health classification using joint acoustic emissions,” unpublished.